

University of Louisville

ThinkIR: The University of Louisville's Institutional Repository

Electronic Theses and Dissertations

5-2008

Comparative linear accuracy of cone beam CT derived 3D images in orthodontic analysis.

April A. Brown 1983-
University of Louisville

Follow this and additional works at: <https://ir.library.louisville.edu/etd>

Recommended Citation

Brown, April A. 1983-, "Comparative linear accuracy of cone beam CT derived 3D images in orthodontic analysis." (2008). *Electronic Theses and Dissertations*. Paper 168.
<https://doi.org/10.18297/etd/168>

This Master's Thesis is brought to you for free and open access by ThinkIR: The University of Louisville's Institutional Repository. It has been accepted for inclusion in Electronic Theses and Dissertations by an authorized administrator of ThinkIR: The University of Louisville's Institutional Repository. This title appears here courtesy of the author, who has retained all other copyrights. For more information, please contact thinkir@louisville.edu.

**COMPARATIVE LINEAR ACCURACY OF CONE BEAM CT DERIVED 3D
IMAGES IN ORTHODONTIC ANALYSIS**

By

April A. Brown B.S.
Masters Candidate in Oral Biology at the
University of Louisville School of Dentistry

A Thesis
Submitted to the Faculty of the
Graduate School of the University of Louisville
In Partial Fulfillment of the Requirements
for the Degree of

Master of Science

Program in Oral Biology
School of Dentistry
University of Louisville
Louisville, Kentucky

May 2008

Copyright 2008 by April A. Brown

All rights reserved

**COMPARATIVE LINEAR ACCURACY OF CONE BEAM CT DERIVED 3D
IMAGES IN ORTHODONTIC ANALYSIS**

By

April A. Brown, B.S., D.M.D.

Masters Candidate in Oral Biology at the University of Louisville School of Dentistry

A Thesis Approved on

March 25, 2008

by the following Thesis Committee:

William C. Scarfe, BDS, FRACDS, MS
Thesis Director

Allan G. Farman, BDS, PhD, DSc
Co-Thesis Director

Anibal Silveira, DDS

James P. Scheetz

DEDICATION

For Lester and Marilyn Sitzes, who have always supported me in all my endeavors. My parents have taught me the value of hard work and sacrifice, and have instilled within me the desire to succeed. I would also like to dedicate this study to my husband, Jesse Brown. None of my accomplishments, including this study, would have been possible without his constant love and support.

ACKNOWLEDGEMENTS

I am greatly indebted to the following for their assistance on this project:

To Dr. William C. Scarfe, thesis director and mentor, for accepting me as a research student, having faith in me and guiding me to the completion of a successful research study. He has sacrificed numerous hours of his personal time to educate and mentor me through not only this research project, but the masters in oral biology program as well. He is truly talented doctor and investigator and I have learned a large wealth of knowledge and wisdom from him. I feel Dr. Scarfe went above and beyond his duty as a mentor in many instances through the support he has provided me at the ULSD. I thank him for all of his direction, and his friendship as well. It was a great privilege conducting this project with him.

To Dr. Allan G. Farman, co-thesis director and mentor, for his continuous guidance and support throughout this study. The opportunity to work with Dr. Farman and learn from such an accomplished, renowned investigator and clinician has been a true privilege and honor. Dr. Farman took a personal interest in my work and other academic endeavors and provided me with exceptional guidance and support. I would like to thank him for his friendship and all of the contributions he has made to this study.

To Dr. James Scheetz, thesis committee member and statistician, for collaborating with us on statistical questions and problems we encountered during the study.

To Dr. Anibal Silveira, thesis committee member and orthodontist, for his support and contribution to my understanding of the orthodontic literature used as the analytical basis in the study.

To Dr. Danielle Periago, orthodontist, for taking the time out of her busy schedule to teach and assist me in using Dolphin software, which was very crucial to the study.

To Dr. Chester Wang, CEO of Dolphin Imaging for provision of software for unrestricted research usage.

To Dr. Mazyar Moshiri, orthodontic resident, for his terrific collaboration with me on this project and providing me with valuable literature.

To Mrs. Barbara Mercer and Mrs. Elaine Lockett, radiologic technologists, for their support and accommodations made in the Radiology and Imaging Sciences Clinic.

ABSTRACT

COMPARATIVE LINEAR ACCURACY OF CONE BEAM CT DERIVED 3D IMAGES IN ORTHODONTIC ANALYSIS

April A. Brown, BS, D.M.D.

May 10, 2008

Objective: To compare the *in vitro* reliability and accuracy of linear measurements between cephalometric landmarks on CBCT 3D images with varying basis projection images to direct measurements on human skulls.

Methods: Sixteen linear dimensions between anatomical sites marked on 19 human skulls were directly measured. Skulls were imaged with CBCT at three settings: 153, 306, and 612 basis projections. The mean absolute error and modality mean of linear measurements between landmarks on 3D images were compared to the anatomic truth.

Results: No difference in mean absolute error between the scan settings was found.. The average skull absolute error between marked reference points were less than the distances between unmarked reference sites.

Conclusion: CBCT measurements were consistent between scan sequences and for direct measurements between marked reference points. Reducing the number of projections for 3D reconstruction did not lead to reduced dimensional accuracy and potentially provides reduced patient radiation exposure.

TABLE OF CONTENTS

	PAGE
DEDICATION.....	iii
ACKNOWLEDGEMENTS.....	iv
ABSTRACT.....	vi
LIST OF TABLES.....	ix
LIST OF FIGURES.....	x
CHAPTER	
I. INTRODUCTION AND LITERATURE REVIEW.....	1
The Limitations of Conventional Film Based Cephalometric Analysis.....	3
Cephalometric Image Accuracy.....	4
Cephalometric Image Clarity.....	5
Advanced Imaging Modalities in Orthodontics.....	9
Computed Tomography.....	10
CBCT in Oral and Maxillofacial Surgery.....	13
CBCT Advantages.....	18
CBCT Applications.....	27
Conventional 3D CT Imaging Accuracy.....	42
Potential of CBCT 3D Cephalometry.....	47
II. STATEMENT OF OBJECTIVES AND HYPOTHESIS.....	49
Study Objectives.....	49
Study Hypothesis.....	50

III. METHODS AND MATERIALS.....	51
Overview.....	51
Sample.....	51
Imaging	57
Data Collection	59
Analysis.....	61
IV. RESULTS	63
V. DISCUSSION	69
VI. SUMMARY AND CONCLUSION	73
VII. REFERENCES	74
VIII. CURRICULUM VITAE.....	82

LIST OF TABLES

TABLE	PAGE
1. Comparison of Maximum Resolution of Imaging Modalities.....	8
2. Comparative Specifications of FDA-Approved CBCT Systems	15
3. Radiation Exposures from CBCT and Other Imaging Modalities.....	21
4. Definition of Mid-Line Craniometric Surface Landmarks	53
5. Definition of Bilateral Craniometric Surface Landmarks.....	54
6. Definition of Linear Distances.....	55
7. Mean Absolute Error (Standard Deviation) of Linear Dimensions.....	64
8. Mean Length (Standard Deviation) of Linear Dimensions.....	67

LIST OF FIGURES

FIGURE	PAGE
1. X-ray Beam Projection Scheme Comparing Conventional or Fan beam CT	10
2. Examples of Current Commercially Available CBCT Units.....	14
3. Axial Orthogonal Image of Phantom.....	18
4. Comparison of Voxel Acquisition Features	23
5. Surface-rendering Reconstruction of i-CAT CBCT Data Set.....	26
6. Application of Maximum Intensity Projection Algorithms	35
7. Visualization of Dental Occlusion from Different Perspectives.....	36
8. Anatomic Landmarks / Planes Used in the Analysis	56
9. Materials Used for Imaging of Skulls	57
10. Skull Positioning for Cone Beam Computed Tomography Scan	58
11. Screen Capture from Dolphin 3D program Demonstrating Segmentation	60
12. Comparison of 3D Shaded Surface Rendered Images	60

CHAPTER I

INTRODUCTION AND LITERATURE REVIEW

Radiographic imaging is an important diagnostic adjunct in the assessment of skeletal and dental relationships for the orthodontic patient. Historically, cephalometric analysis of the maxillofacial complex for orthodontic diagnosis and treatment planning has been determined from linear and angular measurements made on film or digital two dimensional (2D) cephalograms. Over the past decade, cone beam computed tomography (CBCT) specifically for imaging the maxillofacial region has been developed. CBCT is capable of providing sub-millimeter spatial resolution for images of the craniofacial complex with relatively short scanning times (8-70 sec.) and generally lower radiation dosages than ascribed to fan-beam or helical CT imaging methods.[1] Time and dose requirements for CBCT have been suggested to be a similar order of magnitude to other dental radiographic modalities.[2-4]

While CBCT images provide useful information for the orthodontist in regard to the position and location of impacted teeth and other pathologies, datasets can be used to generate both two dimensional (2D) planar projection and three dimensional (3D) surface or volume rendered images for use in orthodontic assessment and treatment planning. CBCT has a number of advantages compared to conventional CT imaging for cephalometric imaging including sub-millimeter resolution and reduced radiation

exposure. Perhaps the most important clinical advantage is that CBCT volumetric datasets can be exported as DICOM files, imported into personal computers and third party software used to provide 3D reconstruction of the craniofacial skeleton. This possibility, and the increasing access of CBCT imaging in orthodontics, is a component of the paradigm that is directing imaging analysis from 2D cephalometry to 3D visualization of craniofacial morphology.[5] The availability of fast scan CBCT now provides multi-planar reformatted (MPR) imaging and the possibility of 3D image reconstruction of the maxillofacial complex with minimal distortion.

The linear accuracy of CBCT derived 2D planar and 3D reconstructions has been previously reported for orthodontic assessment. However the effect of operating parameters on image quality or accuracy directed at reducing dose has not been investigated. There are numerous factors that may affect CBCT image quality including: 1) X-ray beam quality, 2) Detector performance and matrix size, 3) Scan time and number of projections, 4) Completeness of scanning trajectory, 5) Field of view and, 6) Reconstruction algorithm. For most current CBCT units the operator can only adjust parameters 1), 3) and 5). Reducing the number of projections used to reconstruct the volumetric database provides a proportionate reduction in patient radiation exposure but may lead to reduced image quality. As CBCT technology is being applied to 3D orthodontic imaging, the use of techniques to minimize patient exposure and their effect on cephalometric analysis accuracy should be investigated.

Therefore this study was undertaken to compare the in vitro reliability and accuracy of linear measurements between cephalometric landmarks obtained from 3D surface rendered images from maxillofacial CBCT using variable numbers of basis

projection images.

The Limitations of Conventional Film Based Cephalometric Analysis

Since 1931, 2D transmission X-ray images have been used to identify specific skull landmarks from which vertical and antero-posterior skeletal and dental dimensions are derived. These lateral skull radiographs, made under standard projection conditions, are currently the image format used in the analysis of both bony and soft tissue landmarks for orthodontic diagnostic purposes as well as for growth evaluation. Post-treatment cephalograms may also serve to evaluate orthodontic treatment outcome and success. Traditionally, cephalograms have been utilized for their cost and radiation efficiency as well as their ease of use. However, characteristics related to projection geometry such as inherent magnification, superimposition of bilateral anatomic structures and distortion as well as the nature of the detector system can diminish accuracy and reliability in evaluation of craniofacial structures and anomalies.

Digital Cephalometrics

Many conventional film based cephalostats are being replaced by digital systems. The advantages of digital cephalometric imaging versus conventional film based modalities include instantaneous imaging, lack of user and performance sensitive chemical developing processes, facilitated patient communication, ease of storage and retrieval, and the ability to enhance images for size or contrast.[6-8] Currently, three methods are available to produce digital images: digitization of film radiographs, solid state systems (charge-coupled device – CCD; complementary metal oxide semiconductor

– CMOS; thin film transistor - TFT), and photostimulable phosphor systems (PSP).[6-10] Secondary capture through digitization of film radiographs can be achieved using a scanner with a radiograph/transparency adaptor. This method allows for digitization of all film radiographs, however, it is important to note that the quality of scanned images cannot exceed the quality of the original radiograph.[8] CCD detectors are sometimes incorrectly listed in the dental literature as direct digital imaging modalities, because the output is transferred via cables to a computer system and digitized by the frame grabber.[10] They are in fact usually indirect imaging devices as they employ a scintillator in most cases, similar to that used with indirect screen film. CCD is the more costly option for cephalometry in orthodontics. Photostimulable phosphor systems (PSP) are reusable and use an imaging plate that superficially resembles scintillating screens used for traditional extra-oral radiography.[8] These phosphor plates are illuminated by a solid state laser beam to release photoluminescence. The released light is photomultiplied and collected by a digital imaging chip and the signals are then analyzed by the image processor.[6-10]

Image quality in cephalometrics either analog or digital, is determined by two parameters: image accuracy and image quality

Cephalometric Image Accuracy

Cephalometric radiography is based on use of a standardized, reproducible head position in relation to the X-ray source and detector. Ear rods are used to prevent the head from rotating about the vertical, sagittal and transverse axes. A third reference, a nasal positioner, may be used to prevent the nose from rotating about the transverse axis.

However, when the device is used to contact the external auditory meatus and soft tissues of the patient, the head can be incorrectly positioned sagittally, antero-posteriorly, or vertically, as the head can be slightly rotated within the head-holding device.

Due to these errors caused by different positioning of the head, cephalometric linear and angular measurements can vary depending on the different locations of anatomic structures against the central ray. Malkoc *et al.* found that horizontal linear and angular measurements between the horizontal planes on lateral cephalograms were subject to changes from 16.1% to 44.7% with a 14⁰ rotation of the head position. For PA cephalograms, they reported horizontal linear measurements, particularly mandibular length, were subject to a projection error of up to 34.9% with head rotation.[11]

2D transmission cephalometric radiography is subject to inherent geometric differential magnification. All resulting images are magnified, because X-rays do not radiate parallel to the whole part of the projected object. The ratio of magnification varies in the different planes, and hence the image is distorted. In cephalometric radiography, each landmark is not located at the same distance from the focal area of the anode. As a result, changes may be caused in the relationship of the landmarks to one and another on the cephalogram.[12,13]

Cephalometric Image Clarity

Clarity is the term used to describe the visibility of diagnostically important detail in an image. It is determined by two factors; radiographic contrast and image quality. Radiographic contrast is the ability to determine the difference in density between areas of the image. For both analog radiographic film and digital detectors contrast depends on

radiation energy, subject contrast and scatter; however, a fourth element, detector contrast, is also a factor due to inherent dissimilarity between detection systems.

Image quality is defined as the ability to record each point in an object as a point on the detector. For film imaging it is partly determined by radiographic mottle (a feature of the film screen system and film graininess), sharpness and resolution. For digital detectors, seven essential characteristics should be considered: size of active area, signal-to-noise ratio, contrast resolution, spatial resolution, modulation transfer function, quantum efficiency and detective quantum efficiency.[8,15,16]

1. **Active Area:** No standard active areas have been specified for digital imaging systems comparable to the ISO/ANSI standards for the conventional X-ray film. For solid-state extra-oral systems, a narrower receptor is sometimes used for detecting the image and the image is formed via virtual movement. The plates used in storage phosphor systems can be cut to exactly replicate the size of their film counterparts and exposure is similar to cassette motion.
2. **Signal-to-Noise Ratio:** For any imaging system, the useful signal must be compared with background noise which, in analog film, is comparable to the base density plus fog. The base plus fog density for conventional processed film is about 1/20 of the signal density. Both newer CCD and PSP systems outperform film in signal-to-noise ratios (SNS) if base plus fog is considered to be equivalent to SNR. Newer CCD systems exhibit a SNR of approximately 50:1. No matter what the system, all SNRs improve with increased radiation dose.
3. **Contrast Resolution:** In imaging, the ability to separate and distinguish

depends upon contrast between adjacent structures. Using current display monitors, working on the WINDOWS system, the maximum number of gray levels is 242 because the operating system in the past has been reported to use 14 shades and the total supported shades is 256 for an 8-bit display. This is usually the maximum contrast resolution available.

4. **Spatial Resolution:** Resolutions comparable to those of conventional cephalometric radiographs are readily obtained using digital systems/detectors. Table 1 compares detector resolution for a number of currently available conventional film, CCD systems and PSP systems.[14]
5. **Modulation Transfer Function:** MTF is the ability of the detector to transfer the modulation of the input signal at a certain frequency to its output and deals with the display of contrast and object size. MTF is responsible for converting contrast values of different sized objects into contrast intensity levels within the image. Therefore, modulation transfer function (MTF) is a useful measure of true or effective resolution, because it accounts for the amount of contrast and blur over a range of spatial frequencies.[15]
6. **Quantum Efficiency:** The average number of electrons photoelectrically emitted from a photocathode per incident photon of a given wavelength in a phototube. Quantum efficiency (QE) is a quantity defined for a photosensitive device such as photographic film or a charge-coupled device (CCD) as the percentage of photons hitting the photoreactive surface that will produce an electron-hole pair. It is an accurate measurement of the device's sensitivity. It is often measured over a range of different wavelengths to characterize a

device's efficiency at each energy. Photographic film typically has a QE of much less than 10%, while CCDs can have a QE of well over 90% at some wavelengths.[16]

7. **Detective Quantum Efficiency:** Detective quantum efficiency (DQE) refers to the efficiency of a detector in converting incident x-ray energy into an image signal, and is calculated by comparing the signal-to-noise ratio at the detector output with that at the detector input as a function of spatial frequency. It is dependent upon radiation exposure, spatial frequency, MTF, and detector material as well as the quality of the radiation applied. High DQE levels indicate that less radiation is needed to achieve identical image quality, therefore, improved image quality can be obtained by increasing DQE and leaving radiation exposure constant. An ideal detector would have a DQE of 1, indicating that all radiation energy is absorbed and converted into image information. However, in clinical practice the DQE of digital detectors is limited to roughly 0.45 at 0.5 cycles/mm.[15]

Table 1. Comparison of Maximum Resolution of Imaging Modalities

	<i>Analog Film (T-Mat G)</i>	<i>Storage Phosphor</i>	<i>CCD-Based</i>	
<i>Maximum Resolution</i>	<i>OP 100</i>	<i>OP 100 DenOptix</i>	<i>OP 100 DigiPan</i>	<i>Prototype OP 100 D</i>
lp/mm	>5; <6	>5; <6	>4.47; <4.86	>5; <6

Digital cephalometric images have been reported to be diagnostically acceptable for orthodontic treatment planning purposes:[7-10] however, there is a need to further compare various radiographic modes of image capture for cephalometry such as conventional vs. digital radiographs and scanned conventional films vs. digital radiographs.[9]

Advanced Imaging Modalities in Orthodontics

Advanced technologies are those that acquire images using a digital receptor and that provide the possibility of multiple planar reformatting (MPR). In these modalities, multiple images become truly inter-relational in that direct comparisons in multiple planes can be made. Some advanced technologies that are available to image the maxillofacial complex include magnetic resonance imaging (MRI), fan-beam computerized tomography (CT), and Cone Beam Computed Tomography (CBCT). The basis of advanced imaging is the recording of transmitted, attenuated x-rays of an object by a digital receptor to produce a digital image. Digital images are composed of pixels, or picture elements, arranged in a 2-dimensional rectangular grid. Each pixel has a specific size, color, intensity value, and location within an image and is the smallest element of the digitized image. In general, radiographic images use gray color with an intensity value between 8 bits (256 shades of gray) and 16 bits (65,536 shades of gray). The number of pixels per given length of an image (pixels/mm), the number of gray levels per pixel (bits), and the management of the gray levels determine image resolution or the degree of sharpness of the image. A voxel is a three-dimensional stack of bitmapped images, (each voxel having a height, width, and thickness) and is the smallest element of

a three-dimensional image.[18]

Computed Tomography

In addition to utilizing images that are digital, technological advancements now allow dentistry to create images of the maxillofacial region in 3-dimensions. The first 3D imaging technique used in dentistry was computerized tomography (CT). CT units can be divided into two groups based on the acquisition X-ray geometry: fan beam and cone beam (Figure 1). Essentially, the latter method for capturing an image differs from the traditional CT in that it does so by cone beam volumetric tomography. A three-dimensional X-ray beam passes through the object volume investigated. Simultaneously, the beam hits a two-dimensional extended detector and forms a true volumetric acquisition in a single scan (Figure 1).

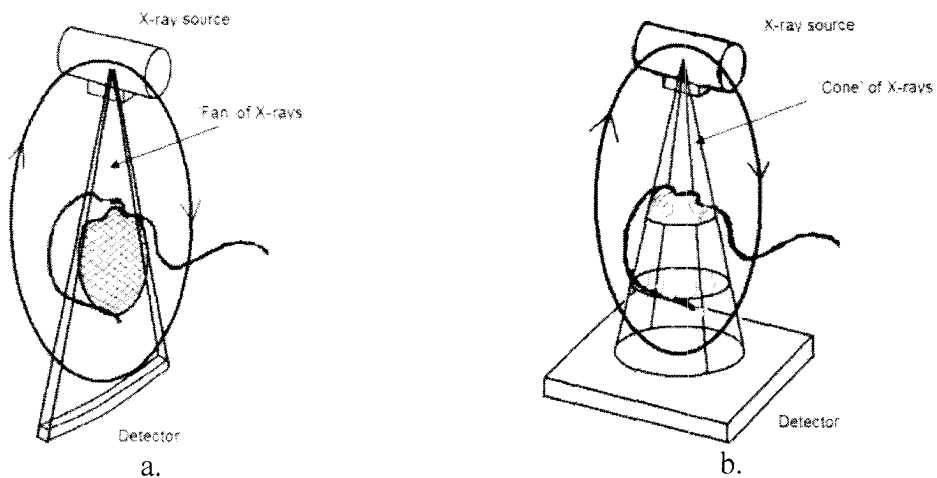


Figure 1. X-ray beam projection scheme comparing conventional or (a.) "fan beam" CT and (b.) cone beam CT (Images courtesy Predag Sukovic, Xoran Technologies, Ann

Arbor, MI USA)

Fan Beam Acquisition

CT scanners consist of an X-ray source and detector mounted on a rotating gantry (Figure 1a). During one rotation of the gantry, the detector detects the flux (I) of x-rays that have passed through the patient. These integrals constitute so-called "raw data" that are then fed into an image reconstruction method that generates cross-sectional images whose pixel values correspond to linear attenuation coefficients. Such machines acquire image data through a thin, broad, fan shaped X-ray beam which is transmitted through the patient. These scanners use a large, arc-shaped detector that acquires an entire projection without the need for translation. This rotate-only design, frequently referred to as "fan-beam", utilizes the power of the X-ray tube much more efficiently than the previous generations. Recent advances in CT include multi-row detectors and spiral scanning. Multi-row scanning allows for the acquisition of several cross-sectional slices at the same time, reducing scanning times. Today's state-of-the-art scanners have 64 rows of detectors. Spiral (helical) scanning incorporates a moving table with the rotating X-ray tube, with the net effect that the X-ray tube describes a helical path around the patient.

Cone Beam Acquisition

CBCT scanners often utilize a 2D flat panel detector (Figure 1b), which allows for a rotation of the gantry to generate a scan of the entire region of interest using a 180 degree or greater rotation (up to two 360 degree rotations), as compared to conventional CT scanners whose multiple "slices" must be stacked to obtain a complete image. In comparison with conventional fan-beam or spiral-scan geometries, cone-beam geometry has higher efficiency in X-ray use, inherent quickness in volumetric data acquisition, and

potential for reducing the cost of CT. Conventional fan-beam scans are obtained by illuminating an object with a narrow, fan-shaped, beam of X-rays. The X-ray beam generated by the tube is focused to a fan-shaped beam by rejecting the photons outside the fan, resulting in a highly inefficient use of the X-ray photons. Further, the fan-beam approach requires reconstructing the object slice-by-slice and then stacking the slices to obtain a 3D representation of the object. Each individual slice requires a separate scan and separate 2D reconstruction. The cone beam technique, on the other hand, requires only a single scan to capture the entire object with a cone of X-rays. Thus, the time required to acquire a single cone-beam projection is the same as that required by a single fan-beam projection. However, since it takes several fan beam scans to complete the imaging of a single object, the acquisition time for the fan beam tends to be much longer than with the cone beam. Although it may be possible to reduce the acquisition time of the fan beam method by using a higher power X-ray tube, this increases the cost and size of the scanner as well as the electric power consumption, thus making the design unsuitable for a compact scanner.

Although CBCT equipment has existed for over two decades, only recently has it become possible to develop clinical systems that are both inexpensive and small enough to be used in operating room, medical offices, emergency rooms, and intensive care. Four technological and application-specific factors have converged to make this possible. First, compact and high-quality flat-panel detector arrays were developed. Second, the computer power necessary for cone-beam image reconstruction has become widely available and is relatively inexpensive. Third, x-ray tubes necessary for cone-beam scanning are orders-of-magnitude less expensive than those required for conventional

CT. Fourth, by focusing on head/neck scanning only, one can eliminate the need for sub-second gantry rotation speeds that are needed for cardiac and thoracic imaging. This significantly reduces the complexity and cost of the gantry.

CBCT in Oral and Maxillofacial Imaging

Currently available CBCT units in the United States are the NewTom QR DVT 3G and VG (Dent-X/Quantitative Radiology s.r.l., Verona, Italy), CB MercuRay (Hitachi Medical Corp., Chiba-ken, Japan), i-CAT Next Generation (Danaher/Imaging Sciences International, Hatfield, PA), Gendex CB 500 (Danaher/Gendex, Chicago, Illinois), Iluma, (Kodak Dental Imaging, Atlanta, GA/Imtec Imaging, Ardmore, OK, USA), Kodak 9000 DS (Kodak Dental Imaging, Atlanta, GA), Galileos, (Sirona Dental Systems, Charlotte NC), 3D Accu-i-tomo – XYZ Slice View Tomograph, (J. Morita Mfg. Corp., Kyoto, Japan), Promax (Planmeca Oy, Helsinki, Finland), E. Woo EPX/Impla and Trio (Vatech Industries, Korea), and Scanora 3D (Soredex, Helsinki, Finland), and PSR 9000N (Belmont/Asahi Roentgen, Kyoto, Japan). All but the five are capable of imaging the skull to include most anthropometric landmarks used in cephalometric analysis (Figure 2)(Table 2). Several additional units are in various stages of testing or FDA approval.

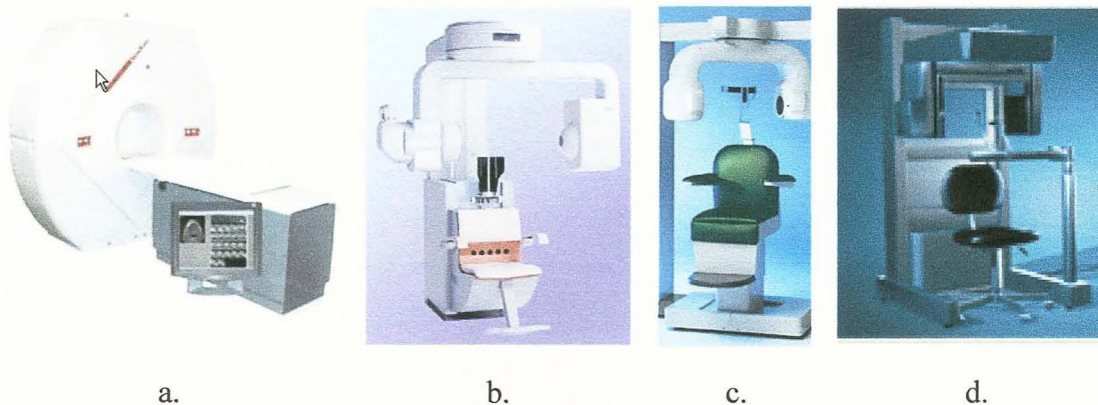


Figure 2: Examples of current commercially available CBCT units for dentomaxillofacial radiology. a. Newtom 9000G (Quantitative Radiology, Verona, Italy) b. CB Mercuray (Hitachi, Medical Corp., Kashiwa-shi, Chiba-ken, Japan) c. 3D Accuitomo – XYZ Slice View Tomograph, (J. Morita Mfg. Corp., Kyoto, Japan) d. i-CAT (Danaher/Imaging Sciences International, Hatfield, PA)

Table 2. Comparative Specifications of Representative FDA-Approved CBCT Systems (Modified from: [19])

<i>Vendor</i>	<i>AFP-Dent-X</i>	<i>J. Morita Mnfr. Corp.</i>	<i>Imaging Sciences Intl.</i>	<i>Hitachi Medical Systems</i>	<i>Kodak Dental Systems</i>	<i>Sirona Dental Systems</i>
CBCT Name	NewTom 3G	3D Accu-i-tomo	iCAT	CB MercuRay	ILUMA Ultra Cone Beam CT Scanner	Galileos
Headquarters	Elmsford, NY	Kyoto, Japan	Hatfield, PA	Tokyo, Japan	Ardmore, OK	Charlotte, NC
Initial FDA/CDRH Approval	March 2001	May 2003	October 2003	October 2003	November 2005	July 2006
Grayscale	12 Bit	12 Bit	12 Bit	12 Bit	14 Bit	12 Bit-sw 16 bit
Foot Print (H x W x D) (meters)	2 x 2 x 0.74	2.08 x 1.62 x 1.2	1.83 x 1.12 x 1.49	2.25 x 1.96 x 1.9	1.06 x 1.42 x 2.15	2 x 1.60 x 1.60
Image Detector	Image intensifier/CCD	Cesium iodide CsI/amorphous silicon flat panel	Cesium iodide CsI/amorphous silicon flat panel	Image intensifier/CCD	127- micron amorphous silicon flat panel	Proprietary Siemens Technology
Rotation per scan	1	1	1 or 2	1	Single 360° Rotation	210° 200 single shots
Patient Positioning	Supine	Seated	Seated	Seated	Seated with rear-head stabilization	Standing/sitting

Table 2 (continued). Comparative Specifications of Representative FDA-Approved CBCT Systems (Modified from: [19])

<i>Vendor</i>	<i>AFP-Dent-X</i>	<i>J. Morita Mnfr. Corp.</i>	<i>Imaging Sciences Intl.</i>	<i>Hitachi Medical Systems</i>	<i>Kodak Dental Systems</i>	<i>Sirona Dental Systems</i>
Pre-Installed Software	NewTom 3G	i-Dixel	Xoran Cat	CBWorks	ILLUMINAVISION3D	SIDEXIS/GALAXIS
Scan time (s)	5.6-36	17	10-4-	9.6	20-40	14
mA	15 max	1-10	3-5	2-15	4-7	5-7
Kv	110 max	60-80	120	120	120	85
Scan diameter (cm)	25	4-6	17	25	17-19	15
Scan height (cm)	15-30	4-6	6-27.4	15-30	10-19	15
Slice width (mm)	0.1-0.5	0.125-2.0	0.2-0.4	0.1-0.5	0.0936-0.4	Voxel size: 150/300 microns

The cone-beamed technique uses a single scan in which the x-ray source and a reciprocating x-ray detector are attached by a "U-" or C-arm and rotate around the patient's head acquiring multiple projection scan images. The field of view (FOV) or area of interest able to be covered is primarily dependent on the detector size (Image intensifier/CCD, CMOS or a:SiTFT field dimensions) and beam projection geometry. While the FOV can be varied by the application of zoomed image reconstruction (e.g. MercuRay [Hitachi, Medical Corp., Kashiwa-shi, Chiba-ken, Japan]) this is usually done at the loss of image resolution.

Data is obtained from a series of multiple single-projection scan images as the x-ray source rotates around the patient's head. The number of images comprising the projection data is determined by the frame rate (number of images acquired per second), the completeness of the trajectory arc and the speed of the rotation. The number of projection scans comprising the data set is variable, depending on the system. The number of projection scans comprising a single scan may be fixed (e.g. Newtom 3G, QR, Inc, Verona, Italy; Iluma, Imtec Inc., Ardmore, OK; Galileos, Sirona AG, Bensheim, Germany, or Promax 3D, Planmeca Oy, Helsinki, Finland) or variable (e.g. iCAT, Imaging Sciences International, Hatfield, PA; PreXion 3D, Terarecon, San Mateo, CA). For example, the i-CAT has a choice of 10 second, 20 second (standard) and 40 second scans in the Classic Generation, and 8 second, 15 second and 20 second scans with the i-CAT Next Generation. For pulsed generator units, the number of basis images produced is roughly proportional to the exposure time reflecting a relatively constant frame rate.

More projection data provides more information to reconstruct the image, allows for greater spatial and contrast resolution, increases the signal-to-noise ratio producing

“smoother” images and reduces metallic artifacts. However this is usually accomplished with a longer scan time, a higher patient dose and longer primary reconstruction time. Reducing the number of projections used to reconstruct the volumetric database provides a proportionate reduction in patient radiation exposure but may lead to reduced image quality (Figure 3). As CBCT technology is being applied to 3D orthodontic imaging, the use of techniques to minimize patient exposure and their effect on cephalometric analysis accuracy should be investigated.

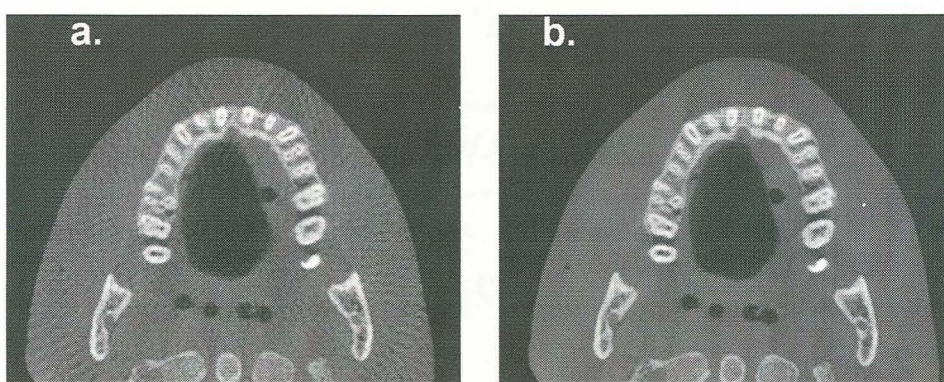


Figure 3: Axial orthogonal image of phantom demonstrating the effect of image quality of increasing the number of projections used to construct a volumetric dataset from (a.) 306 projections (20s scan) to (b.) 612 projections (40s scan).

CBCT Advantages

Because CBCT provides images of high contrasting structures well, it is extremely useful for evaluating osseous structures. Combined with the limitation of FOV, CBCT is therefore well suited towards the imaging of the craniofacial area. Currently, limitations exist in the application of this technology for soft tissue,[23, 24] but efforts are being directed towards the development of software algorithms to improve signal-to-

noise and optimize available contrast.

The utilization of CBCT technology in clinical practice provides a number of potential advantages compared with conventional CT related to the beam limitation, scan time reduction, and image display. Specifically the advantages of CBCT are as follows [19]:

- 1) **Variable FOV.** Collimation of the CBCT primary x-ray beam enables limitation of the X-radiation to the area of interest. For most (but not all) CBCT systems an optimal FOV (field of view) can be selected for each patient based on suspected disease presentation and the region to be imaged. For example, radiographic investigation of the mandible can be performed by selection of an appropriate FOV. This functionality provides additional dose savings by limiting the irradiation field to fit the FOV, with a resulting exposure reduction to the patient.
- 2) **Sub-millimeter resolution.** Maxillofacial diagnostic CBCT units all use megapixel solid state devices for x-ray detection providing a minimal voxel resolution of $< 0.25\text{mm}$ isotropically, exceeding the specifications of commonly used multi-slice CT systems in terms of spatial resolution.
- 3) **High speed scanning.** Because CBCT acquires all projection images in a single rotation, scan time can be reduced enormously. In the fan-beam CT system, particularly in high resolution, each thin slice thickness can take up to several tens of seconds. However, various CBCT systems can scan an entire head in 10 seconds or less. While faster scanning times usually mean less number of projections from which to reconstruct the MPR images, motion

artifact due to subject movement is reduced. Reconstruction times vary depending on FOV and scanning speed.

- 4) **Dose reduction.** Preliminary reports indicate that CBCT patient absorbed dose can be significantly reduced when compared to conventional CT used with manufacturer recommended sequences.[25] The Newtom 9000 system (Quantitative Radiology, Verona, Italy) also has an automatic exposure control device which selects the starting intensity of the x-ray beam, depending on the size of the patient, and modifies the anodic current according to the density of the transversed tissues (maximum value 15mA). This reduces the patient absorbed dose to approximately that of a film-based periapical survey of the dentition [26-28] or 1-7 times that of a single panoramic image (varying with the panoramic system used).[29, 30] Depending on bone density, a traditional CT exposes the patient to approximately 6-8 times that amount when evaluating either the maxilla or mandible [29] and 15 times the amount of CBCT exposure when imaging both the maxilla and mandible.[31] Table 3 compares radiation exposures from CBCT and other imaging modalities.

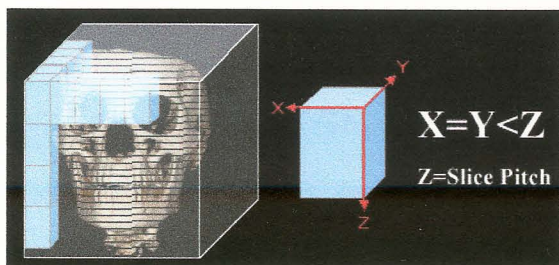
Table 3. Radiation Exposures from CBCT and Other Imaging Modalities (Modified from: [19])

<i>Machine & Technique</i>	<i>Effective Dose (μSv) using 1990 ICRP</i>	<i>Dose in single panoramic multiples</i>	<i>Dose in days per capita background</i>	<i>Dose in % medical CT equivalent</i>	<i>Dose % annual per capita background</i>
NewTom 3G full (12") FOV	45	7	4	2.1	1.2
NewTom 3G w/ chin tilt & thyroid shield	28	4	3	1.3	0.8
CB MercuRay full (12") FOV 10 mA-100kV	477	74	48	22.7	13.2
CB MercuRay P (9") FOV	289	45	29	13.8	8
CB MercuRay I (6") FOV 125 (maxillary)	169	26	17	12	4.7
CB MercuRay I (6") FOV w/ chin tilt	125	19	12	5.9	3.5
iCAT full (12") FOV	135	21	13	6.4	3.7
iCAT w/ chin tilt & thyroid shield	57	9	6	2.7	1.6
Panoramic (OrthoPhos Plus DS)	6	1	1	0.3	0.3
CT maxilla & mandible	2100	385	243	100	58.3
CT maxilla	1400	164	103	100	38.9
Galileos	Pending	Pending	Pending	Pending	Pending

5) ***Voxel isotropy***. The smallest element of a volumetric dataset is the voxel.

Voxels have a dimension of thickness as well as the height and width of a 2-dimensional pixel. Voxel representation and therefore resolution are dependent on lateral slice thickness, determined principally by the matrix size of the detector and longitudinal slice thickness (body axis), which in conventional CT is determined by slice pitch, a function of gantry motion. Therefore, conventional CT data is obtained anisotropically, where axial voxel dimensions are equal, but where coronal dimensions are greater and are determined by slice pitch, usually a 1mm minimum (Figure 3a). Therefore, spatial resolution in the longitudinal slice (body axis direction) is poorer than that of lateral slice. On the other hand, the CBCT uses a 2D detector and the same high resolution is obtained in the longitudinal slice (body axis direction) and lateral slice (transverse direction). This voxel representation is known as *isotropic* (Figure 4b). Because of this characteristic, coronal multi-planar reformatting (MPR) of CBCT data has the same resolution as axial data.

a. Anisotropic Voxel



b. Isotropic Voxel

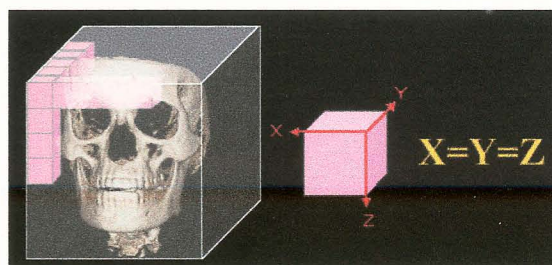


Figure 4: Comparison of voxel acquisition features on conventional “fan beam” CT (a.) and “cone beam” CT (b.)

- 6) ***Real time analysis and manipulation.*** Although conventional CT data is inherently digital, images are supplied to referring clinicians as fixed format, hard copies on film transparencies. CT image algorithms necessary to reformat the data require the computing power of workstations. While such data can be “converted” and imported into proprietary programs for use on personal computers (e.g. Simplant and Simplant CMF: Materialise, Ann Arbor, MI, USA; Procera: Nobel Biopharma, Sweden)) this process is expensive and requires an intermediary stage that potentially extends the diagnostic phase. Reconstruction of CBCT data is performed natively by a personal computer. In addition, availability of software to the user, not just the radiologist, is available either via direct purchase or innovative “per use” license from the various vendors (e.g. Danaher/Imaging Sciences International). Further, because the original data is isotropic, it can theoretically be re-orientated such that the patient’s anatomic features are re-aligned. At least one manufacturer has incorporated this capability into both

their acquisition and viewer software (Imaging Sciences International).

Finally, the availability of cursor-driven measurement algorithms provides the clinician with an interactive capability for real-time dimensional assessment.

7) ***Display modes unique to maxillofacial imaging.*** CBCT software can reconstruct the projection data to provide as many as 512 coronal, sagittal and axial MPR frames. Common to all standard viewing layouts are usually preset options providing display of coronal, sagittal and axial MPR frames. Basic manipulations include zoom or magnification, window/level, the capability to add annotation and measurement algorithms. Some proprietary software is capable of advanced imaging processing functions including:

- a. Oblique MPR such as linear oblique MRP (useful for TMJ assessment) or curved oblique MPR providing a “panoramic” image.
- b. Cross-sectional imaging provides sequential multi-slice images usually perpendicular to the “panoramic” MPR, useful in implant site assessment or lateral oblique MPR which has application in the assessment of the TMJ.
- c. Variable slice thickness adjustments for oblique MPR images provide the clinician with the possibility of producing undistorted plain radiograph projection-like images. One example is the creation of a cephalometric plane projection, either sagittally or coronally. This is developed by increasing the slice thickness of a mid sagittal MPR plane to the width of the head (130-150mm) to produce an image composed of the summed voxels, an image which has been referred to as “Ray Sum”.

This image can be exported and analyzed using third party proprietary cephalometric analysis software. This functionality may potentially reduce the need for additional radiographic exposure. Oblique MPR images along the curve of the dental arch with slice thickness comparable to the in-focus image layer of panoramic radiographs (15-35mm) can also be individually created to provide a “panoramic” radiograph customized for each patient. However, unlike conventional panoramic radiographs, these MPR images are undistorted and are free from projection artifacts.

- d. Maximum intensity projection (MIP). This is a three dimensional volume rendering technique which is used to visualize high-intensity structures within volumetric data. At each pixel, the highest data value encountered along a corresponding viewing ray is depicted. In combination with oblique MPR and selection of wide slice thickness, this technique is capable of providing 3D surface images. This is particularly useful in cephalometric radiography.
- e. Surface and volume rendering algorithms are available with some software which provides three-dimensional reconstruction and presentation of data that can be interactively adjusted (Figure 5).

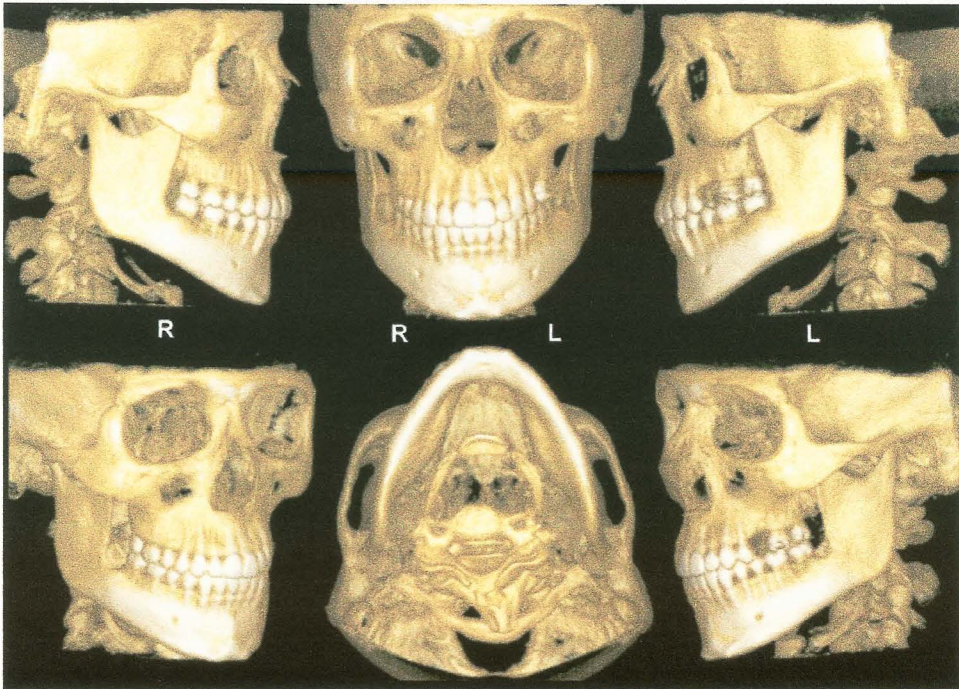


Figure 5. Surface-rendering reconstruction of i-CAT CBCT data set (3DVR, Allovision, Greenville, SC) produces interactive volumetric image that can be manipulated to display bony surfaces of maxillofacial complex from various standard orientations.

f. Previously unavailable for viewer use, numerous image enhancement algorithms are now able to optimize image presentation. While the diagnostic efficacy of the application of these algorithms is yet to be studied, preliminary investigations indicate that sharpening and edge filters show the greatest potential in refining anatomic structures for interpretation.

8) ***Variable acquisition modes.*** Many, but not all, units are capable of variable scanning fields of view (FOV) from large FOV capable of imaging the entire

craniofacial complex (currently up to 13.2cm with i-CAT and 19cm with CB MercuRay to limited FOV for specific diagnostic tasks. The Iluma at the time of this research was limited to one full FOV.

CBCT Applications

The advent of CBCT technology has paved the way for the development of relatively small and inexpensive CT scanners dedicated for use in dento-maxillofacial imaging. Manufacturers' web sites provide numerous examples illustrating the value of CBCT in evaluating the position of impacted teeth, supernumerary teeth, maxillary sinus position (in reference to maxillary molars), mandibular canals, and lingual nerves. Maxillofacial applications of CBCT imaging have also been reported for oral and maxillofacial surgery.[34-38] implantology, [39-42] and craniofacial assessment in orthodontics.[43-48] A number of researchers have reported high dimensional accuracy of maxillofacial CBCT in measurement of facial structures.[42,49] Other examples of this modality's uses include surgical assessment of pathology, and preoperative/postoperative assessment of craniofacial fractures.[24,28,33]

Applications in Orthodontics

In orthodontics CBCT imaging has current and potential applications in the diagnosis, assessment and analysis of patients with maxillofacial orthodontic and orthopedic anomalies.

In diagnosis, CBCT provides numerous display modalities that can assist the assessment of numerous dental conditions of concern in orthodontics including impacted

and supernumerary teeth. The exact position of impacted teeth and their relationships to adjacent roots or other anatomical structures (eg. the mandibular canal) can be comprehended, so that surgical exposure and subsequent movement can be planned. Some of the most significant potential gains from the introduction of CBCT in orthodontics are the ability of integration of information. Instead of looking at individual diagnostic records—the panoramic radiograph, the cephalogram and its concurrent analysis, the dental models and the patient photographs—a single volume that contains all of this information is now available allowing for a unique appreciation of the inter-correlations between all planes and structures. Image integration, particularly three dimensional imaging, may help to overcome a number of inherent deficiencies in orthodontic treatment planning by providing adequate visualization of anatomical structures.[51, 53] These include assessment of:

- 1) Temporomandibular joint condition prior to treatment particularly if related to condylar trauma and structural development during growth
- 2) Osseous structural conditions in the sagittal, vertical and transverse plane
- 3) Alveolar bone width of available bone for buccolingual movement of teeth (i.e. arch expansion or labial movement of incisors) and evaluation of fenestrations and dehiscence on the buccal and lingual surfaces.
- 4) Tooth inclination and torque: 3D evaluation of the axial inclination of teeth might provide information to supplement that obtained from models.
- 5) Root resorption: Current CT machines could have too low resolution to detect early stages of root resorption due to orthodontic movement, but advances in technology might permit this in the future.

- 6) Soft tissue relationships: Lip length is currently measured on lateral radiographs, but mouth width is not. Three-dimensional data could provide information on the relationship of the corners of the mouth to the underlying dentition. Also, cheek thickness and cheek prominence are soft tissue variables that could be investigated in relation to dental arch width and facial esthetics.
- 7) Tongue size and posture: Volume measurements of the tongue could provide a more objective assessment of size, to aid in the diagnosis of open bites and arch-width discrepancies.
- 8) Airway assessment: Volume measurements of the airway could assess patency, especially in patients who are suspected of mouth breathing, adenoid hypertrophy, or sleep apnea. Nasal morphology and turbinates can be clearly seen in CT scans.
- 9) Patients requiring surgery and those with syndromes and clefts: Surgical planning for such patients can benefit from 3D imaging. 3D data are especially helpful in patients with asymmetry, where true dimensions can be measured, without the problems of magnification or distortion, from which our customary 2D projections suffer. In patients with clefts, bone and soft-tissue defects can be understood much better.

There is an increasing desire in orthodontics to integrate the images of all functional elements, both hard and soft tissue, in the assessment of patients with maxillofacial anomalies. Currently, this is performed using a combination of photographic and radiographic images and study models. Due to the fact that

orthodontics involves assessment of hard tissue and soft tissue interactions, such as the effects of tooth movement on esthetics and on functional elements such as occlusion and TMJ, it is highly desirable to have one imaging modality that provides images of all existing elements therefore leading to a better assessment of the interactions present.

Traditionally, conventional cephalometric projections such as the lateral cephalogram, posterior anterior, and submentovertex were used individually or in combination to provide two dimensional representations of structures in three planes of space. There was no single imaging technique readily available to the orthodontist that provided accurate representation of all osseous aspects of the TMJ complex and associated structures until the recent commercialization of CBCT.

Hilgers *et al.* studied CBCT multi-planar reformatted projections for TMJ examination to compare the accuracy of linear measurements of the TMJ and related structures with similar measurements made using conventional cephalograms and with the anatomic truth. Using a digital caliper, the investigator measured linear dimensions between 11 anatomic sites to assess the anatomic truth for 25 dry human skulls. All skulls were imaged using i-CAT CBCT and digital cephalograms (PSP) were made in all three orthogonal planes (lateral cephalometric, posterior anterior, and submentovertex). Linear measurements were made on seven custom CBCT reconstructions and the digital cephalograms. Results showed that all CBCT measurements were accurate; however, three of five lateral cephalometric (LC) measurements, four of five posterior anterior (PA) measurements, and four of six submentovertex (SMV) measurements varied significantly from the truth. Intra-observer CBCT measurements were highly reliable compared to the anatomic truth, and significantly more reliable than measurements made

from LC, PA, and SMV images. The authors conclude that custom oblique MPR reconstructions using CBCT provides accurate and reliable linear measurements of mandibular and TMJ dimensions.[54]

Since cephalometric radiology was developed, numerous analyses have been proposed to facilitate communication between practitioners and to describe how individual patients vary from norms derived from other studies. None the less, current cephalometric analyses are two dimensional diagnostic renderings derived from a three dimensional structure. Cephalometric measurements made on 2D radiographs are subject to projection, landmark-identification, and measurement errors.[56-58] The major source of cephalometric error is landmark-identification, which is influenced by many factors such as the quality of the radiographic image, the precision of landmark definition, the reproducibility of the landmark location, the operator, and the registration procedure. Although some cephalometric landmarks are located in the midsagittal plane, many are located at different depth fields leading to increased distortion errors.[56-58] In addition, in lateral cephalometry, it is difficult to determine the difference between right and left sides for superimposition of images, and the sides have different enlargement ratios. It is also difficult to detect deformities in the midfacial area and reading films is difficult due to the superimposition of cranial structures.[59] Despite the potential errors innate to this technique, cephalometric radiographs are still widely used and, in many cases are essential in the diagnosis and treatment of the patient.

To compensate for the drawbacks of 2D measurements, many techniques have been developed. These techniques include the orientator,[60] the coplanar stereometric system,[61] the multiplane cephalometric analysis,[62] the basilar multiplane

cephalometric analysis.[63] and the biplanar cephalometric stereoradiography.[64]

Since the mid 1970s, 3D analyses and related procedures in orthodontics have been attempted through several different approaches.[56] There have been three dimensional cephalometrics proposed that use a combination of lateral and frontal cephalograms. These methods rely on the identification of the same point on both radiographs and the implementation of geometry to calculate the point three dimensionally. These approaches, however, are not truly three dimensional and have obvious limitations in that the accuracy depends on a correct correspondence between the landmark locations on the two radiographs, and points not visible on both radiographs cannot be used.[51] Advances in the use of 3D imaging software have permitted important changes in the perception of 3D craniofacial structures.[56] CBCT produces a lower radiation dose than spiral CT and is comparable to conventional radiographs.

Because of its volumetric data, CBCT allows secondary reconstructions, such as sagittal, coronal, and para-axial cuts and 3D reconstructions of various craniofacial structures.[34,43,56] Unlike the traditional cephalometric radiograph, the CBCT produces images that are anatomically true (1:1 in size) 3D representations, from which slices can be displayed from any angle in any part of the skull and provided digitally on paper or film. Other reasons for the implementation of 3D cephalometry include:[59]

- 1) actual measurements can be obtained
- 2) a spatial image of the craniofacial structures can be produced
- 3) the 3D image can be rotated easily by changing the rotational axis
- 4) the inner structures can be observed by removing the outer surfaces
- 5) various anatomical areas can be observed independently by changing the

density

According to Hajeer there are numerous benefits of 3D imaging in orthodontics including: pre- and post-orthodontic assessment of dentoskeletal relationships and facial esthetics, auditing orthodontic outcomes with regard to soft and hard tissues, 3D treatment planning and 3D soft and hard tissue prediction. 3D orthodontics also offers efficiency in archiving 3D facial, skeletal and dental records for treatment planning, research and medico-legal purposes.[55] Some authors indicate that three dimensional CBCT images may be useful in the assessment of growth and development.[18,20,35-37,50]

However, many practitioners are accustomed to working with traditional two dimensional cephalograms and may be hesitant to turn to 3D. however, 2D conventional measurements do not have to be abandoned when moving to 3D implementation. Three dimensional data can be rendered as a 2D projection resembling a radiograph allowing traditional analyses to be completed, and customary cephalometric points can also be digitized in 3D on the volumetric rendering itself.[51] Halazonetis believes that the push at implementation of 3D imaging in cephalometrics will lead to an introduction of new landmarks and new analyses which also incorporate advances from related fields, such as geometric morphometrics.[51]

Several CBCT systems permit reconstructions that are comparable with traditional cephalometric projections. Recently, Farman and Scarfe reported a methodology for generating simulated lateral cephalometric images from CBCT using “ray-sum” multiplanar reformatted (MPR) volume reformation.[65] The authors describe a methodology in which existing CBCT image data sets acquired using a 20-second

exposure cycle were used to create two dimensional projection images. The three methods of acquisition involved:

- 1) Scout method: exporting the lateral scout radiograph taken initially to confirm the patient's position, which only provided a lateral cephalogram,
- 2) Basis image method: selecting the individual lateral and anteroposterior basis images with the least anatomic discrepancies between the right and left sides corresponding to lateral and posteroanterior cephalometric projections and
- 3) Ray-sum method: manipulation of the volumetric data set allowed for the development of cephalometric images in all three orthogonal planes. The ray-sum method includes two dimensional cephalometric reconstructions that were developed by increasing the slice thickness of each plane, hence providing an image composed of the summed voxels, or a ray-sum image.

The authors indicate that the major difference between the scout or basis image method, or conventional cephalometric images, and the ray-sum method, is that ray sum image projections are orthogonal and have equal magnification between the beam's entrance and exit sides of the patient. The authors were able to produce slices equal to the dimension of the chosen voxel resolution, thus removing anatomic superimposition of landmarks and allowing for more precise definition of bony landmarks. The authors suggest that the use of 3D surface rendering techniques such as maximum intensity profile algorithms (Figure 6) and volume rendering (Figure 7) will redefine orthodontic treatment planning due to the ability to view 3D volumes of the maxillofacial complex from any plane.

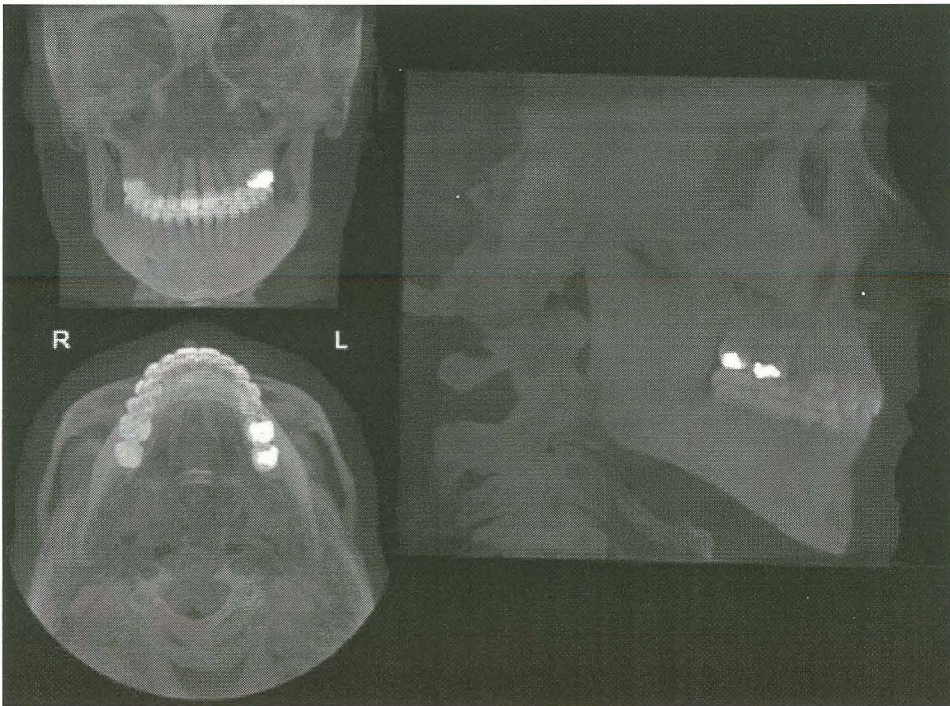


Figure 6. Application of maximum intensity projection algorithms to ray-sum projections show relationships of numerous elements (eg, angulation of tooth roots in alveolar bone) because of their transparent nature. Ray-sum projections provide surface representation of CBCT volumetric data as posteroanterior, submentovertex, and lateral skull images.[65]

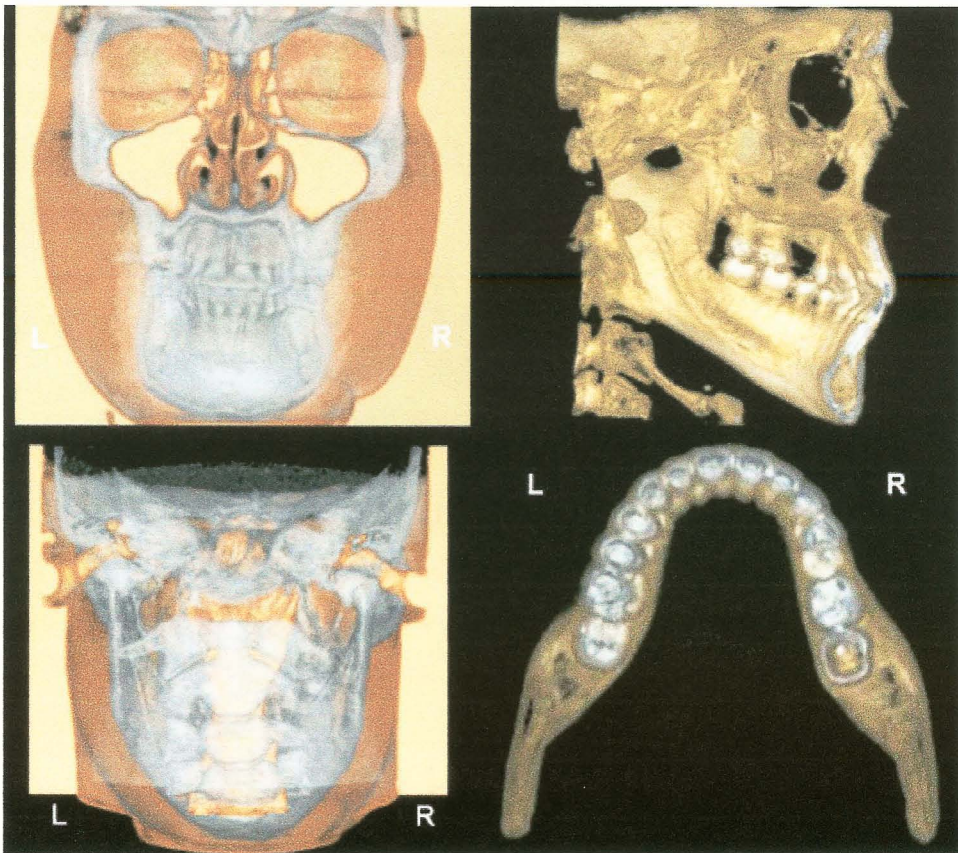


Figure 7. Integration of hard- and soft-tissue volumetric data are achieved through surface- and volume-rendering techniques. Visualization of dental occlusion from different perspectives can be achieved via production of surface images of selected maxillofacial structures.[65]

In a recent study, Moshiri *et al.* showed that data from full field scanners can be used to generate simulated cephalometric images.[66] This observational cross-sectional *in vitro* study was conducted to compare the accuracy of linear measurements made on planar images from photostimulable phosphor based cephalograms and two dimensional (2D) simulated lateral cephalograms derived from full field cone beam computed tomography (CBCT) with direct measurements made on human skulls. The investigator

measured the linear dimensions between 15 anatomical landmarks on 23 dentate dry human skulls using a digital caliper to provide nine orthodontic linear measurements (S-N, Ba-N, M-N, ANS-N, ANS-PNS, Pog-Go, Go-M, Po-Or and Go-Co). The skulls were stabilized and imaged with CBCT with a single 360⁰, 20s, 0.4mm voxel resolution scan. Three 2D simulated cephalometric projections were created: 1) Scout (S), 2) “ray-sum” reconstructed (RS) and 3) basis projection single frame (F) images. Conventional lateral cephalograms (LC) were acquired using a Quint Sectograph and a storage phosphor imaging plate system. TIFF Images were imported into a cephalometric analysis program (Dolphin Imaging Cephalometric and Tracing Software, Chatsworth, CA, USA) and a single observer computed the linear measurements between landmarks and compared them to the anatomic truth. The results showed that the ICC for LC was significantly less than for skull and all CBCT derived modalities. Statistical differences between modalities were found for all measurements except Po-Or ($p=0.27$). For S-N, Ba-N, ANS-PNS and N-M, values for lateral cephalogram measurements were significantly different from actual dry skull dimensions, whereas CBCT values did not differ from the dry skull measurements. All modalities provided significantly different measurements for Pog-Go and Go-M. For ANS-N and Go-Co all CBCT measurements were significantly less than lateral cephalogram measurements. In addition for Go-Co, measurements from scout images were significantly different from actual dimensions. The study concluded that for most measurements in the sagittal plane, simulated 2D lateral cephalometric projections from CBCT are more accurate than lateral cephalogram images. The authors also add that while cephalometric images generated from single CBCT basis projections provide added accuracy in cephalometric analysis, there was no additional advantage in using ray sum

images generated from the CBCT volumetric dataset.

Adams *et al.* conducted a study to evaluate and compare traditional 2D cephalometric analysis to a 3-D imaging system with regard to accuracy in recording the anatomical truth as defined by physical measurements taken using a calibrated caliper.[67] The study used nine dried human skulls to locate thirteen skeletal landmarks both by traditional 2D cephalometry as well as the three dimensional approach. The high average intra-class correlation (0.995), variance (.054 mm²), and standard deviation (SD \pm 0.237 mm) as averaged over 76 measurements derived from precision calipers, using the predetermined 13 skeletal landmarks, established these physical measurements as the gold standard for comparison of the two radiographic methods. The measurements from the 2D model indicated higher variability, with a larger mean standard deviation (6.94 mm) compared with the 3D measures (0.54 mm). The 2D analysis lacked precision as compared with the 3D analysis (points clustered within 0.5 mm). As compared to the gold standard, the ranges between the two systems demonstrated a much larger magnitude of potential error inherent in the 2D system. According to the study, when comparing the actual distance of anatomical distances as measured on a human skull to the measurements derived from a 2D or 3D model, the 3D method is more accurate and precise than the 2D. According to the authors, "Evaluating distances in 3D space with a 2D image grossly exaggerates the true measure and offers a distorted view of craniofacial growth."

Chidiac *et al.* compared measurements from human skulls and their images from lateral and PA cephalometric radiographs and CT scanograms on thirteen adult skulls. They were unable to reveal any statistically significant differences between mean angular

values on cephalometric radiographs and CT views. For sagittal distances, the highest correlation was between the direct measure of condylion-to-pogonion and its radiographic image ($r= 0.73$). Correlations between radiographic and skull transverse measures were higher ($0.46 < r < 0.80$) than the corresponding skull vs. CT measures ($0.06 < r < 0.38$). CT and CR images are 2D slices and projections, respectively, of 3D structures. They found that radiographic images have a distortion (approximately 8%) that brings Co-Pg closer to its anatomic distance, inadvertently contributing to better clinical planning, particularly in orthognathic surgery. The pattern of distortion of PA images was in opposite directions for CR and CT views. They concluded that cephalograms and CT scanograms are close in depicting angular relations of structures, but they differ in the accuracy of imaging linear measurements, because the location and size of an object within the imaged 3D structure varies with both records.[68]

Most recently, Chan *et al.* compared eight measurements [(sagittal (Sella-Nasion, ANS-PNS), transverse (biorbital, bicoronoidal, and palatal width) and vertical (upper, lower, and posterior facial height)] between 12 commonly used craniometric landmarks made directly on five dry skulls to traditional cephalometry and CBCT (Hitachi CB MercurRay system) using three fields of view (6", 9", and 12"). Intraoperator analysis for skull, CBCT and cephalometric measurements showed good correlation ($r>0.93$). Both cephalometric and all CBCT measurements showed high correlation ($r>0.96$) and no statistical significant difference when compared to skull measurements. The average absolute difference between cephalometric and skull measurements was 3.34 ± 4.55 mm. Comparing skull to CBCT measurements, 6", 9", and 12" FOV images showed differences of 0.53 ± 0.46 mm, 0.48 ± 0.44 mm, and 0.46 ± 0.45 mm respectively. They

concluded that CBCT measurements showed reliability and more linear measurement accuracy than cephalometry and that CBCT linear measurement accuracy improved as voxel size decreased.[69]

Although recent studies have shown that CBCT derived images are accurate in regard to linear cephalometric measurements,[66,67] the current challenge for clinicians is to understand and interpret 3D imaging, because there is currently no specific way to analyze these 3D images, and interpretation limitations still exist.[56] Lagravere *et al.* proposed a reference landmark for use in three dimensional cephalometric analysis with 3-dimensional volumetric images.[56] CBCT scans were obtained on 10 patients, all using the same imaging protocol of having the patient lie down with the Frankfort horizontal plane perpendicular to the floor. Images were converted into DICOM format and then rendered into volumetric images using AMIRA software. The investigators used the sagittal, axial, and coronal slices and the 3D image reconstruction for landmark positioning. A point located equidistant to the points in the centers of each foramen spinosum (ELSA) was established as the reference point ($x=0, y=0, z=0$ coordinates). Traditionally used cephalometric landmarks were located on the volumetric images and coordinates of the different landmarks were determined with respect to that reference. Coordinates of ELSA were registered in a datasheet in the form of x, y, and z dimensions for the 10 subjects measured at three independent times. Present statistical tests do not consider 3D data values, therefore in order to find the intraexaminer reliability, it was necessary to convert all 3D values (x, y, and z) to a sole value using the Delta E formula obtained from the Commission Internationale de l'Eclairage $L^*a^*b^*$ color systems (Vienna, Austria). This system was applied because both use similar Cartesian coordinate

systems. The intra-examiner reliability was determined to be $\kappa = 0.998$. Other cephalometric landmarks were then located in different parts of the images where linear and angular measurements could be determined. ELSA as an $x = 0, y = 0, z = 0$ reference point in 3D images was used because the location of the foramina spinosum was shown to have a low identification error in both the vertical and horizontal planes. The reason in choosing this landmark was twofold: 1) it is a small circle when viewed axially and is easy to locate by using the condyle and the glenoid fossa as guides, and 2) published literature has demonstrated that most of the cranial base growth (>85%) occurs in a child's first 5 years with only minor changes after that age. The authors state that although 3D imaging is a new type of auxiliary examination in orthodontics, no validated method of describing change exists. Most clinicians analyze these images by visually identifying the structures seen without exact measurements or other quantitative analysis. The authors conclude that because ELSA has high intrareliability that it is an adequate reference point for 3D cephalometric analysis.

Although three-dimensional imaging provides volumetric images that can be compared to reality in a 1 to 1 ratio, there is no validated method to describing change with this modality, because most clinicians simply analyze the images with no exact measurements or quantitative analysis.[70] By establishing a precise and reliable instrument for analyzing images produced by 3-D technology, clinicians may have new possibilities for determining changes produced by certain types of orthodontic treatment. In a subsequent study, Lagravere *et al.* propose certain landmarks and planes to standardize 3D cephalometric image orientation.[70] CBCT scans were obtained on 10 adolescents free from craniofacial anomalies. Images were converted into DICOM format

and then rendered into volumetric images using AMIRA software. The investigators used the sagittal, axial, and coronal slices as well as the 3D reconstruction of the images for landmark positioning. To determine orientation planes, the reference point ELSA from the previous study was located, then points located at the superior-lateral border of the external auditory meatus (SLEAM) bilaterally and on the mid-dorsum of foramen magnum (MDFM) were located. Coordinates (in mm) were established for these three points with respect to ELSA and intrareliability values were determined by using the intraclass correlation coefficient for all four points. The axial-horizontal plane (x-y plane) was then determined by using both superior external auditory meatus and ELSA; the sagittal-vertical plane (z-y plane) was formed by ELSA and mid-dorsum foramen magnum perpendicular to the x-y plane. Because all points are located on structures that are not significantly affected by growth after 5 years of age these planes are adequate for standardizing the orientation of 3D images and eliminating the possibility of different results when using other landmarks or structures that might be influenced by growth or treatment. With these planes, the effect of the patient's head position during image acquisition for analysis would be eliminated. The authors conclude that ELSA, rSLEAM, lSLEAM, and MDFM have high intrareliability when locating them with 3D images. The x-y and z-y planes formed by the respective points are an adequate way to standardize the orientation of 3D images.

Conventional 3D CT Imaging Accuracy

The clinical applicability of 3D CT has been evaluated in many studies, and a number of authors have investigated the accuracy of reconstruction software using

conventional fan beam derived data sets.[71-73] Recent studies have indicated that there is a high degree of accuracy of 3D reconstructions[74-76] with differences between measurements and actual dimensions being 2mm to 3mm.[77,78]

The accuracy of craniometric measurements in 3D surface rendering technique has previously been reported,[75] and recently a new 3D CT volume rendering protocol *in vitro* and *in vivo* was established regarding the mental foramen, testing the accuracy and precision of the system.[79] However, there had previously been no report concerning the validation of the soft tissue and the corresponding bone craniometric measurements using specific computer system tools in association with a 3D-CT volume rendering technique. Therefore, Cavalcanti *et al.*[74] investigated the precision and accuracy of anthropometric measurements using 3D conventional (spiral) CT volume rendering by imaging 13 cadaver heads and compared the dimensional accuracy of 10 linear measurements on 2D and 3D reconstructed images performed by two radiologists with those obtained using a spatial digitizer. They used craniofacial measurements including Al–Al (Nasal breadth), G–Op (Skull length), N–Me (Facial height), N–Ns (Nasal height), Po–Al (Camper’s plane), Po–G (Distance between Po and G), Po–Me (Distance between Po and M), Po–N (Distance between Po and N), Po–Ns (Distance between Po and Ns), and Zy–Zy. They found no statistically significant differences between interobserver and intraobserver measurements or between imaging and physical measurements in both 3D-CT protocols. The standard error was found to be between 0.45% and 1.44% for all the measurements in both protocols, indicating a high level of precision. Furthermore, there was no statistically significant difference between imaging and physical measurements ($P \geq 0.01$). The error between the mean actual and mean 3D-

based linear measurements was 0.83% for bone and 1.78% for soft tissue measurements, demonstrating high accuracy of both 3D-CT protocols. The authors concluded that the new methodology allowed for a qualitatively high 3D resolution in both bone and soft tissue parameters. They also express that the anthropometric measurements in 3D-CT were considered to be accurate and precise for craniofacial applications.

Recently, Swennen *et al.* developed a new voxel-based 3D cephalometry method.[80] From a single computed tomography data set, virtual lateral and frontal cephalograms are computed and linked with both hard and soft tissue 3D surface representations, allowing the setup of a precise and reproducible 3D cephalometric reference system[81.82] and reliable and accurate definition of 3D cephalometric hard and soft tissue landmarks[83.84]. Voxel based 3D cephalometry was developed and validated by using spiral multi-slice CT (MS-CT) data.[85] Statistical analysis showed that MS-CT 3D cephalometry is highly accurate and reliable with intraobserver measurement errors as low as 0.88, 0.76, and 0.84 mm for horizontal, vertical, and transverse orthogonal measurements, respectively. Interobserver measurement error was also low: 0.78, 0.86, and 1.26 mm for horizontal, vertical, and transverse orthogonal measurements respectively. Squared correlation coefficients showed high intraobserver and interobserver reliability.[86.82] The authors state that MS-CT cephalometry is a powerful craniofacial measurement tool with several advantages:[80]

- 1) truly volumetric 3D depiction of hard and soft tissues of the skull
- 2) real size (1:1 scale) and real time 3D cephalometric analysis
- 3) no superimposition of anatomic structures
- 4) high accuracy and reliability

- 5) the setup of a biological meaningful 3D cephalometric reference system for cross-sectional and longitudinal analysis of craniofacial changes.
- 6) MS-CT Cephalometry is a major improvement over conventional 2D cephalometry. however, some drawbacks do exist:[80]
- 7) horizontal positioning of the patient during record taking falsifies the position of the soft tissue facial mask
- 8) lack of a detailed occlusion due to artifacts
- 9) limited access for the routine craniofacial patient because of higher cost
- 10) higher radiation exposure than other craniofacial x-ray acquisition systems

Most recently Park *et al.*[59] have described organized, methodological

approaches to cephalometric analysis of 3D CT images. Axial images of 30 subjects were taken using CT Hispeed Advantage (GE Medical System, Milwaukee) and reconstructed into 3D models using Vworks 4.0 (Cybermed, Seoul, Korea). Horizontal, midsagittal, coronal, maxillary, mid-maxillary, mandibular, and mid-mandibular planes were all established. 19 Landmarks were first designated on the 3D surface model, and their positions were verified in multiple planar reformat mode. then the Vworks 4.0 and Vsurgery (Cybermed) programs were used to measure the 3D models. The following measurements were determined:

- 1) Zygoma: facial index, midface angle, and Bc point
- 2) Maxilla: canting, rotation, divergence, A-point, and PNS point
- 3) Mandible: canting, rotation, divergence, body length, ramal height, gonial angle, chin prominence, internal ramal inclination, external ramal inclination, lateral ramal inclination, B-point, Pog point, Me point, and mandibular facial

width

- 4) Facial convexity (indicates the protrusive state of Bc, A, B, and Pog to the coronal plane)

The results show that cephalometric measurements of the subjects were comparable with the normal Korean averages (t test, $p \leq .01$) and no statistically significant differences were found. All landmarks were reproducible, and there was no significant intra-examiner error between the 2 sessions ($p \geq .01$). The authors do suggest that there are some limitations when using conventional 3D CT as a diagnostic tool. Relatively large errors in the vertical position (z-coordinate) compared with the anteroposterior (y-coordinate) and transverse (x-coordinate) positions were found. The authors state that these errors can be overcome if thin slices are used during the reconstruction. The authors also express that high cost and radiation dose of conventional CT are major disadvantages, and can be improved upon by using cone beam CT, which offers a dose similar to the range of a conventional dental radiographic examination (40 to 50 μ Sv). In addition, in some craniofacial deformities, Orbitale or Porion are deviated, therefore, points in the horizontal plane should not be used as the reference plane. This limitation can also be overcome by using CBCT, in that CBCT can take an image in the natural head position, and the horizontal reference plane can be parallel to the floor, which is not influenced by Porion and Orbitale. The authors conclude that valuable information can be obtained from a 3D CT reconstruction, and that good treatment results can be obtained with a more precise diagnosis, and the continuous development of 3D analysis will provide more accurate data on a patient.[59]

Potential of CBCT 3D Cephalometry

The application of CBCT technology has allowed the development of a new generation of commercial volumetric dentofacial imaging acquisition systems.[59] CBCT scanners allow image acquisition of a large part of the craniofacial complex with only a 360° rotational sequence, and with dedicated CB reconstruction algorithms a CT data volume is obtained. [86] These scanners focus mainly on bony imaging, leading to a significant decrease in radiation dose. Interesting advantages of CBCT 3D cephalometry for the future include:[80]

1. Reduced radiation exposure
2. Natural shape of the soft tissue facial mask because of the vertical scanning procedure (i-CAT, CB Mercuray)
3. Reduced artifacts at the level of the occlusion
4. Increased access for the routine dentofacial patient because of in-office imaging (sufficiently compact to be installed in orthodontic and oral surgery outpatient clinics and private practices)
5. Reduced cost

Current limitations of CBCT 3D cephalometry include the scanning volume and positional dependency of the image value of a structure in the field of view of the scanner.[80] The NewTom 3G, i-CAT, and CB Mercuray CBCT scanners all have a scanned volume that is sufficient enough for the setup of the anatomic Cartesian 3D cephalometric reference system and 3D cephalometric hard and soft tissue analyses that do not involve the calvarium or complete ears. However, the 3D Accu-i-tomo and NewTom 9000 systems are not suitable for 3D cephalometry methods due to scanning

volumes that are too small.[80] In CBCT systems, the image value of an organ is dependant upon the position in the image volume. Hence, x-ray attenuation of CBCT acquisition systems currently produces different HU values or radiographic densities for similar bony and soft tissue structures in different areas of the scanned volume. An example of this would be that dense bone has a specific image value at the level of menton, but the same bone has a significantly different image value at the level of the cranial base.[80] Vannier states that when new developments in the synthesis and optimization of CBCT reconstruction algorithms allow the full exploitation of the potential of area detectors in CBCT, that CBCT will provide even more important benefits in craniofacial imaging.[44] Therefore it is suggested that improvements in both CB reconstruction algorithms and post-processing will solve or reduce this problem soon.[80]

In conclusion, CBCT derived 3D cephalometry has a number of potential advantages for cephalometric imaging including sub-millimeter resolution, reduced radiation exposure, and inclusion of soft tissue profile. Perhaps the most important clinical advantage is that CBCT volumetric data can be exported as DICOM files and imported into personal computer based software to provide 3D reconstruction of the craniofacial skeleton. This possibility and the increasing access of CBCT imaging in orthodontics is a component of the paradigm that is directing imaging analysis from 2D cephalometry to 3D visualization of craniofacial morphology.[5] The availability of fast scan CBCT now provides an alternate imaging modality capable of providing a 3D representation of the maxillofacial complex with minimal distortion using multi-planar reformatted (MPR) images.

CHAPTER II

STATEMENT OF OBJECTIVES AND HYPOTHESES

Study Objectives

The aim of this research is to compare the *in vitro* reliability and accuracy of linear measurements between cephalometric landmarks obtained from 3D surface rendered images from maxillofacial CBCT using variable numbers of basis projection images. This is important because while maxillofacial CBCT imaging is now being used to produce 3D images these are being acquired at appreciably higher doses than conventional digital cephalometric images. If CBCT protocols involving reduced number of images can provide comparable 3D images then this can lead to substantial patient radiation dose reduction.

The specific aims of this study were to compare the:

1. reliability of linear measurements made on CBCT derived 3D surface rendered volumetric images generated using Dolphin 3D software (Chatsworth, CA) from various numbers of projections to direct measurements made on a sample of 19 human skulls.
2. accuracy of linear measurements made on CBCT derived 3D surface rendered volumetric images generated using Dolphin 3D software (Chatsworth, CA) from various numbers of projections to direct measurements made on a

sample of 19 human skulls.

Study Hypothesis

Null Hypotheses (H_0)

1. There is no difference in the reliability of linear measurements made on CBCT derived 3D surface rendered volumetric images generated using Dolphin 3D software (Chatsworth, CA) from various numbers of projections to direct measurements made on a sample of 19 human skulls.
2. There is no difference in the accuracy of linear measurements made on CBCT derived 3D surface rendered volumetric images generated using Dolphin 3D software (Chatsworth, CA) from various numbers of projections to direct measurements made on a sample of 19 human skulls.

Alternate Hypotheses (H_1)

1. There is a difference in the reliability of linear measurements made on CBCT derived 3D surface rendered volumetric images generated using Dolphin 3D software (Chatsworth, CA) from various numbers of projections to direct measurements made on a sample of 19 human skulls.
2. There is a difference in the accuracy of linear measurements made on CBCT derived 3D surface rendered volumetric images generated using Dolphin 3D software (Chatsworth, CA) from various numbers of projections to direct measurements made on a sample of 19 human skulls.

CHAPTER III

METHODS AND MATERIALS

This observational cross-sectional *in vitro* experiment was approved by the Institutional Human Remains Committee, Department of Anatomical Sciences and Neurobiology at our university.

Sample

The sample consisted of 19 dry dentate human skulls with a stable and reproducible occlusion, presence of a full permanent dentition and similar skull size. No demographic data was available on the studied human remains and the sample was not identified by age, gender or ethnicity. Fifteen anatomical landmarks, were identified on each skull using an indelible marker providing a total of 24 anatomical sites. A limited selection of 15 surface craniometric landmarks, of which nine were bilateral (Table 4 and 5), were chosen to provide representative linear dimensions in vertical, transverse and horizontal planes. Operational definitions were developed as elaborations or modifications of those presented by previous authors. [77, 91] The dimensions between these specific points provided sixteen linear distances commonly used in lateral cephalometric orthodontic analysis (Table 6; Figure 8). To establish the true distances between the selected anatomic points, measurements were made by the principal author

and research associate (MM) three times independently using an electronic digital caliper (27-500-90, GAC, Bohemia, NY). The mean of the measurements served as anatomic truth.

To provide soft-tissue equivalent attenuation, two latex balloons filled with water were placed in the cranial vault prior to imaging. To separate the mandibular condyle from the temporal fossa, a 1.5 mm thick styrofoam wedge was placed in the joint space between the glenoid fossa and the condylar head. For all images, the teeth were placed in centric occlusion (maximum intercuspation) and the jaws were held closed by bilateral metal springs. A custom plastic head holder, with a polyvinyl chloride pipe extension for placing into the foramen magnum, was constructed to support the skulls during imaging (Figure 9).

Table 4. Definition of Mid-Line craniometric surface landmarks used in the cephalometric analysis.

<i>Landmark</i>	<i>Abbreviation</i>	<i>Definition</i>
<i>Nasion</i>	<i>NA</i>	<i>A mid-sagittal point on the bridge of the nose at the most superior point of fronto-nasal suture</i>
<i>Anterior Nasal spine</i>	<i>ANS</i>	<i>Most anterior limit of the floor of the nose, at the tip of the anterior nasal spine in the mid-sagittal plane</i>
<i>A Point</i>	<i>A</i>	<i>The deepest (most posterior) on the anterior curvature of the maxilla in the mid-sagittal plane</i>
<i>Posterior Nasal Spine</i>	<i>PNS</i>	<i>The most posterior extent of the hard palate in the mid-sagittal plane.</i>
<i>B Point</i>	<i>B</i>	<i>The deepest (most posterior) point on the anterior curvature of the mandible in the mid-sagittal plane</i>
<i>Menton</i>	<i>ME</i>	<i>Most inferior point along the curvature of the chin in the mid-sagittal plane</i>

Table 5. Definition of Bilateral craniometric surface landmarks used in the cephalometric analysis.

Landmark	Abbreviation	Definition
<i>Medio-orbitale</i>	<i>MO</i>	<i>The point on the medial orbital margin that is the most distal point along the fronto-maxillary suture</i>
<i>Lateral piriform aperture</i>	<i>NC</i>	<i>The most lateral aspect of the piriform aperture</i>
<i>Antegonion</i>	<i>AG</i>	<i>The most superior point in the antegonial notch</i>
<i>Gonion</i>	<i>GO</i>	<i>A point on the inferior surface of the mandible which lies midway along the curvature between the ramus and the body.</i>
<i>Zygomatic arch</i>	<i>ZA</i>	<i>A point at the most lateral surface of the zygomatic arch near the zygomatico-maxillary suture</i>
<i>Condylion</i>	<i>CO</i>	<i>The most superior point of the condylar head</i>
<i>Zygomaticofrontal medial suture point</i>	<i>Z</i>	<i>The point at the medial margin of the orbital rim at the zygomaticofrontal suture</i>
<i>Mental foramen</i>	<i>MF</i>	<i>The most disto-lateral point of the mental foramen on the buccal surface of the mandible</i>
<i>Jugale; Maxillare</i>	<i>J</i>	<i>The most inferior point in the curvature of the lateral contour of the maxillary alveolar process</i>

Table 6. Definition of linear distances commonly used in lateral cephalometric orthodontic analysis.

<i>Definition</i>	<i>Type</i>	<i>Abbreviation</i>
Nasion - Menton	Vertical	Na-Me
Condylion – Gonion (Lt & Rt side)	Vertical	Co-Go
Zygomaticofrontal medial suture point – Antegonion (Lt & Rt side)	Vertical	Z-Ag
Nasion – Anterior Nasal Spine	Vertical	Na-ANS
Anterior Nasal Spine – Posterior Nasal Spine	Vertical	ANS-PNS
Nasion – A Point	Vertical	Na-A
Nasion – B Point	Vertical	Na-B
Gonion (Rt) – Gonion (Lt)	Horizontal	Go-Go
Mental Foramen (Rt) – Mental Foramen (Lt)	Horizontal	Mf–Mf
Medio-Orbitale (Rt) – Medio-Orbitale (Lt)	Horizontal	Mo-Mo
Zygomatic Arch (Rt) – Zygomatic Arch (Lt)	Horizontal	Za-Za
Nasal Canal (Rt) – Nasal Canal (Lt)	Horizontal	NC- NC
Zygomaticofrontal medial suture point (Rt) - Zygomaticofrontal Medial suture point (Lt)	Horizontal	Z-Z
Jugale (Rt) - Jugale (Lt)	Horizontal	J-J

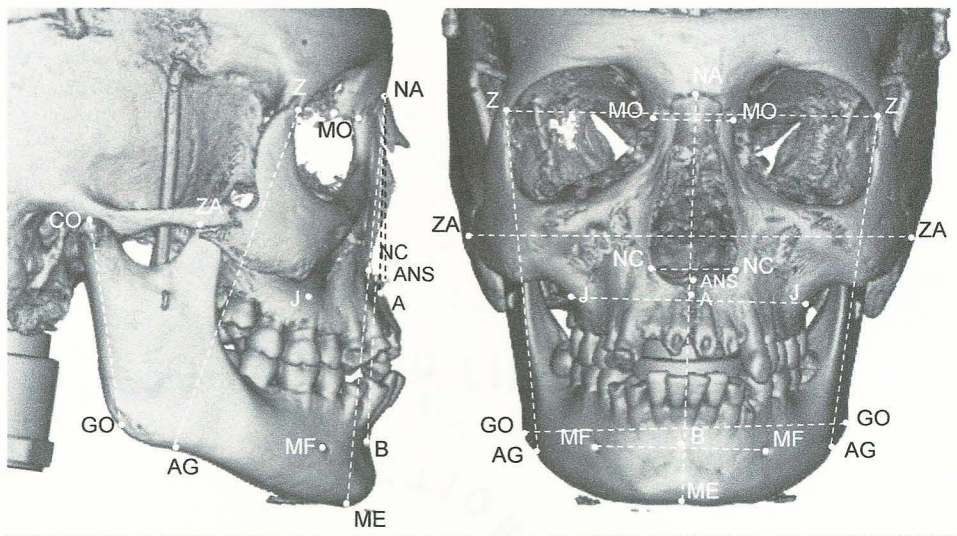


Figure 8. Anatomic landmarks / planes used in the analysis are shown on lateral (left) and frontal (right) projections of 3D shaded surface rendering. Linear distances were determined for the following dimensions: Na-Me = Nasion – Menton; Co-Go (Lt & Rt side) = Condylion – Gonion; Z-Ag (Lt & Rt side) = Zygomatico-frontal medial suture point – Antegonion; Na-ANS = Nasion – Anterior Nasal Spine; ANS-PNS = Anterior Nasal Spine – Posterior Nasal Spine; Na-A = Nasion – A Point; Na-B = Nasion – B Point; Go-Go = Gonion (Rt) – Gonion (Lt); Mf-Mf = Mental Foramen (Rt) – Mental Foramen (Lt); Mo-Mo = Medio-Orbitale (Rt) – Medio-Orbitale (Lt); Za-Za = Zygomatic Arch (Rt) – Zygomatic Arch (Lt); NC-NC = Nasal Canal (Rt) – Nasal Canal (Lt); Z-Z = Zygomatico-frontal medial suture point (Rt) – Zygomatico-frontal medial suture point (Lt); J-J = Jugale (Rt) - Jugale (Lt).



Figure 9. Materials used for imaging of skulls: gloves filled with water, skull holder and foam wedges, and skull.

Imaging

Cone beam CT images were acquired using a maxillofacial CBCT unit capable of a full head scan (iCAT Classic, Imaging Sciences International, Hatfield, PA, USA). The device was operated at 3-8 mA (pulse-mode) and 120 kV using a high frequency generator with fixed anode and 0.5 mm nominal focal spot size. The anterior symphyseal region of the mandible of each skull was inserted into the chin holder and vertical and horizontal lasers were used to position the skull. The specimen was oriented by adjustment of the chin support until the mid-sagittal plane was perpendicular to the floor and the horizontal laser reference coincided with the intersection of the posterior maxillary teeth and alveolar ridge (Figure 10).

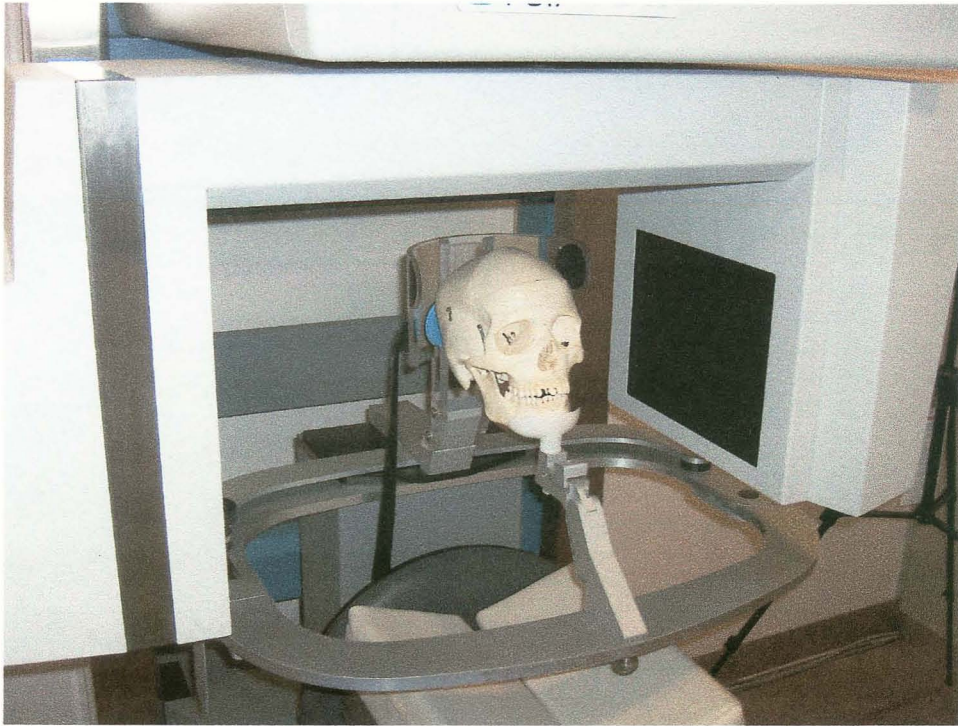


Figure 10. Skull positioning for cone beam computed tomography scan

Full trajectory (360°) rotational scans were then made for each skull with a 17.0 cm (diameter) x 13.2 cm (height) field of view and at 0.4mm voxel resolution using XoranCat acquisition software (Xoran Technologies, Ann Arbor, MI, version 1.7.7). Three scan settings were used producing volumetric datasets comprised of different numbers of basis projections. a) CBCT 10: 10 second, 153 projections, b) CBCT 20: 20 second, 306 projections and, c) CBCT 40: 40 second, 612 projections.

Primary reconstruction of the data was automatically performed immediately after acquisition and took between 1 to 5 minutes depending on the scan setting. Secondary reconstruction occurred in “real time” and provided contiguous color correlated perpendicular axial, coronal and sagittal 2D MPR slices, with isotropic 0.4mm voxels in

each orthogonal plane.

Data Collection

The CBCT data was exported from the XoranCat software in DICOM multi-file format and imported into Dolphin 3D (V.10, Dolphin Imaging, Chatsworth, CA) on the same computer. All constructions and measurements were performed on a 20.1-inch flat panel color active matrix TFT (FlexScan L888, Eizo Nanao Technologies Inc., Cypress, CA) screen with a resolution of 1600 x 1200 at 85 Hz and a 0.255 mm dot pitch, operated at 24 bit. This software is capable of generating 3D shaded surface display volumetric rendered images using the entire volumetric data set. This involves generating an image of the skull by manually adjusting the threshold of visible pixel levels, a process called segmentation (Figure 11). This process provided for 3D renderings which demonstrated visual differences, depending on the number of basis images used in the reconstruction (Figure 12).

Next the surface rendered volumetric image was reoriented such that the Frankfort horizontal was parallel to the lower border of the screen display in both sagittal and coronal projections. Then the cephalometric landmarks were located and marked on the surface rendered volumetric image. The Dolphin 3D software allowed 3D CBCT measurements from different views using rotation and translation of the rendered image. Landmarks were identified by using a cursor-driven pointer. This was performed by a sequence of pre-set volumetric orientations.

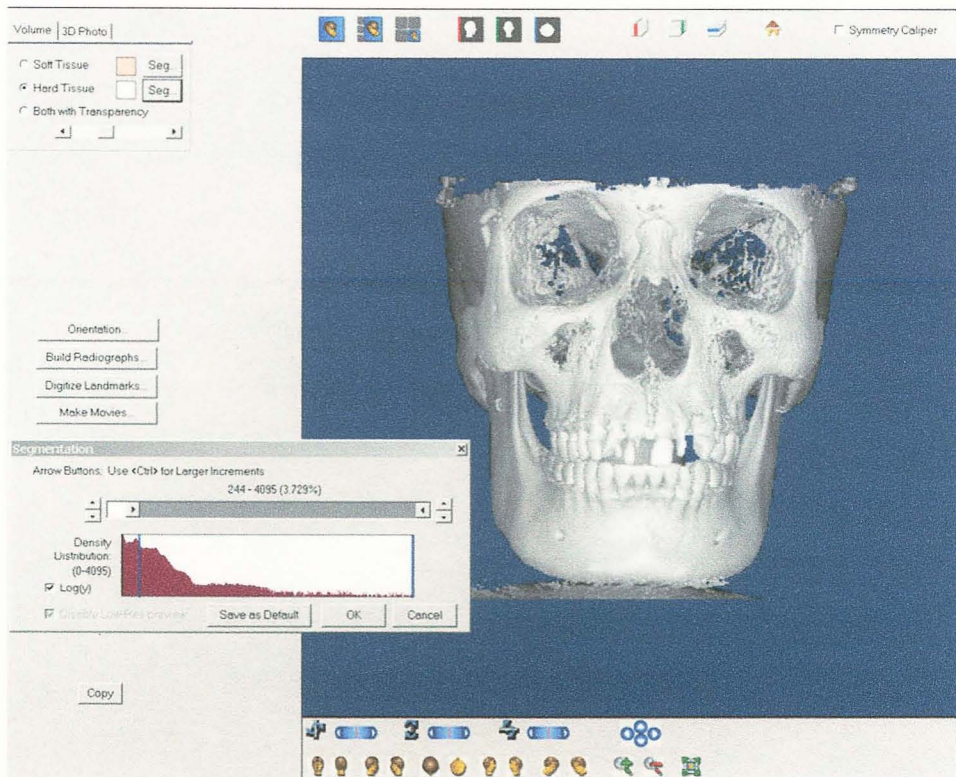


Figure 11. Screen capture from Dolphin 3D program demonstrating the segmentation process. The hard tissue volume segmentation is selected (upper left) and using the segmentation cursor (lower left), the displayed gray level of the voxels is dynamically altered to provide the most realistic appearance of the skull with minimal loss of cortical bone due to thin structures and minimal superimposition of artifacts and soft tissue.

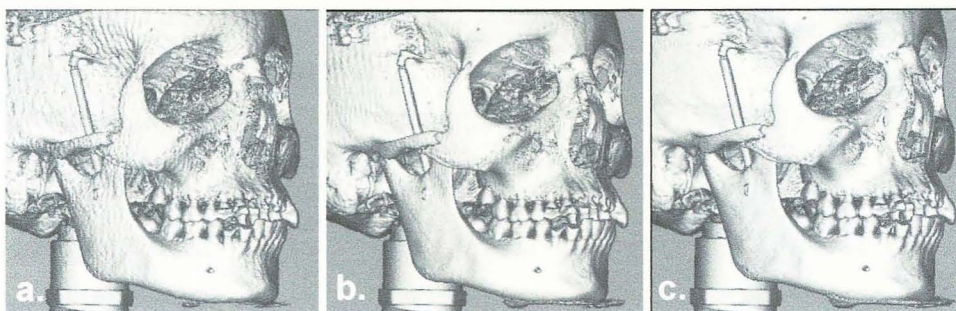


Figure 12. Comparison of 3D shaded surface rendered images from (a.) CBCT 10, (b.) CBCT 20 and, (c.) CBCT 40.

Finally measurements between specific landmarks were made. A custom analysis within the program was developed that directed the observer to identify specific anatomic landmarks on the images which were identified by using a cursor-driven pointer. For the version of the software version used, points and planes were unnamed. Therefore it was necessary to select points to identify a linear plane. This was performed in a specific sequence such that specific linear measurements corresponded to certain cephalometric planes and were calculated by the proprietary measurement algorithm implemented by the Dolphin software. In this way the resulting analysis provided specific linear measurements which could be exported as text data. This procedure was repeated three times by the principal author.

Analysis

All measurements from the Dolphin custom cephalometric analysis were exported with the “data” export function into a text document. The text documents were entered, rearranged and data subsequently exported into a Microsoft Excel 2007 (Microsoft, Redmond, WA, USA) database. Means and standard deviations of three independent repeats of the measurements performed by consensus were calculated for each skull and used as anatomic truth. For each imaging mode the average of three triplicate independent analyses from the PI was used. The data files were coded for use with statistical software ((SPSS V.12, Chicago, Il, USA). To determine intra-observer reliability, absolute mean error (\pm s.d.) were calculated for triplicate measurements. Mean dimensions of the three repeated measurements within modality groups were compared with the repeated measure General Linear Model using the Wilks Lambda multivariate

test ($p \leq 0.05$) and the Sidak adjustment for multiple comparisons.

CHAPTER IV

RESULTS

Table 7 shows the mean absolute intra-rater measurement error for 3D CBCT and skull measurements. Overall mean percentage measurement error for anatomic skull dimensions ($.45\text{mm} \pm .17\text{mm}$; Range: $.1\text{mm} \pm .08\text{mm}$ to $.75\text{mm} \pm .71\text{mm}$) was significantly lower than the error for CBCT 10 ($P < .001$)(Mean diff. = $.44\text{mm}$), CBCT 20 ($P < .001$)(Mean diff. = $.38\text{mm}$) and CBCT 40 ($P < .001$)(Mean diff. = $.32\text{mm}$). There were no differences between CBCT modalities. For ten of the sixteen measurements at least one of the CBCT mean absolute errors was significantly higher than direct skull measurements using the methods described.

Table 7. Mean absolute error (mm) and standard deviation (\pm s.d.) of Orthodontic Linear Dimensions for skulls compared to CBCT derived shaded surface 3D renderings reconstructed from 153 (CBCT 10), 306 (CBCT 20) and 612 (CBCT 40) basis projections.

<i>Measurement</i>	<i>Modality</i>								<i>Significance</i>	
	<i>Skull</i>		<i>CBCT 10</i>		<i>CBCT 20</i>		<i>CBCT 40</i>			
	<i>Mean</i>	<i>s.d.</i>	<i>Mean</i>	<i>s.d.</i>	<i>Mean</i>	<i>s.d.</i>	<i>Mean</i>	<i>s.d.</i>	<i>F</i>	<i>p</i>
Na-Me ^a	0.44 ^a	0.24	0.96 ^a	0.48	0.77	0.63	0.87 ^a	0.52	7.08	0.003
Co-Go (rt)	0.53	0.40	1.19	1.31	0.89	0.60	0.78	0.53	2.17	0.131
64 Co-Go (lt)	0.64	0.60	0.99	0.51	0.88	0.64	0.72	0.54	1.53	0.25
Z-Ag (rt)	0.75	0.71	0.81	0.40	0.87	0.50	0.91	0.68	0.24	0.87
Z-Ag (lt) ^b	0.40 ^b	0.25	0.79 ^b	0.37	1.09 ^b	0.87	0.92 ^b	0.50	8.68	0.001
Na-ANS ^c	0.32	0.21	0.58 ^c	0.36	0.32 ^c	0.21	0.46	0.32	3.43	0.042
ANS-PNS ^d	0.71 ^d	0.55	1.18 ^d	0.50	0.88	0.47	1.00	0.71	3.05	0.059
Na-A ^e	0.36 ^e	0.32	1.28 ^e	1.08	1.05 ^e	0.59	1.06 ^e	0.36	10.37	<.001
Na-B ^f	0.39 ^f	0.23	0.93 ^f	0.53	0.80 ^f	0.46	0.69 ^f	0.39	12.7	<.001
Go-Go	0.48	0.45	0.79	0.50	0.76	0.46	0.68	0.48	2.2	0.128

Table 7 (continued). Mean absolute error (mm) and standard deviation (\pm s.d.) of Orthodontic Linear Dimensions for skulls compared to CBCT derived surface 3D renderings reconstructed from 153 (CBCT 10), 306 (CBCT 20) and 612 (CBCT 40) basis projections.

<i>Measurement</i>	<i>Modality</i>								<i>Significance</i>	
	<i>Skull</i>		<i>CBCT 10</i>		<i>CBCT 20</i>		<i>CBCT 40</i>			
	<i>Mean</i>	<i>s.d.</i>	<i>Mean</i>	<i>s.d.</i>	<i>Mean</i>	<i>s.d.</i>	<i>Mean</i>	<i>s.d.</i>	<i>F</i>	<i>p</i>
Mental f.–Mental f ^g	0.51 ^g	0.32	1.16 ^g	0.93	1.29 ^g	0.81	0.98 ^g	0.51	11.4	<.001
Mo-Mo ^h	0.37 ^h	0.32	0.97 ^h	0.66	1.33 ^h	1.15	0.95 ^h	0.37	15.79	<.001
Za-Za ⁱ	0.10 ⁱ	0.08	0.46 ⁱ	0.25	0.49 ⁱ	0.17	0.52 ⁱ	0.10	27.68	<.001
NC- NC ^j	0.19 ^j	0.13	0.63 ^j	0.27	0.62 ^j	0.28	0.60 ^j	0.19	21.49	<.001
Z-Z ^k	0.40 ^k	0.22	0.68	0.44	0.56	0.35	0.62 ^k	0.29	3.48	0.04
J-J	0.57	0.41	0.73	0.42	0.61	0.42	0.57	0.57	0.52	0.676
Mean^l	0.45^l	0.17	0.88^l	0.24	0.83^l	0.28	0.77^l	0.19	8.24	0.138

Modality differences between skull and CBCT measurements ^aSkull abs. mean error less than CBCT 10/40 (p<.001; p=.02), ^bSkull abs. mean error less than CBCT 10/20/40 (p=.005; p=.024; p=.002), ^cCBCT 10 greater than CBCT 20 (p=.024), ^dCBCT 10 greater than CBCT 40 (p=.05), ^eSkull abs. mean error less than CBCT 10/20/40 (p=.01; p=.002; p=.006), ^fSkull abs. mean error less than CBCT 10/20/40 (p=.001; p=.003; p=.044), ^gSkull abs. mean error less than CBCT 10/20/40 (p=.02; p=.005; p=.01), ^hSkull abs. mean error less than CBCT 10/20/40 (p=.025; p=.19; p=0), ^{i,j}Skull abs. mean error less than CBCT 10/20/40 (p<.001), ^kSkull abs. mean error less than CBCT 40 (p=.038). ^lOverall skull abs. mean error less than CBCT 10/20/40 (p<.001).

Table 8 provides comparison of mean linear measurements obtained from each of the 3D CBCT reconstructions and actual skull dimensions. For 6 dimensions, there were no differences between 3D CBCT and actual skull measurements. All CBCT scan settings produced lower measurements than skull values for 6 dimensions (Na-Me, Z-Ag_{rt/lr}, ANS-PNS, Za-Za, NC-NC)(mean difference 3.1mm ± .12mm). For Na-ANS and Z-Z, CBCT 20/40 dimensions were less than skull measurements (mean difference .56mm ± .07mm) whereas for mental f.-mental f. CBCT 10/40 dimensions were less than skull measurements (mean difference 2.96mm ± .18mm). For Mo-Mo, CBCT measurements were greater than actual skull measurement (mean difference 3.4mm ± .12mm).

Table 8. Mean length (mm) and standard deviation (\pm s.d.) of Orthodontic Linear Dimensions for skulls compared to CBCT derived shaded surface 3D renderings reconstructed from 153 (CBCT 10), 306 (CBCT 20) and 612 (CBCT 40) basis projections.

<i>Measurement</i>	<i>Axis</i>	<i>Modality</i>								<i>Significance</i>	
		<i>Skull</i>		<i>CBCT 10</i>		<i>CBCT 20</i>		<i>CBCT 40</i>			
		<i>Mean</i>	<i>s.d.</i>	<i>Mean</i>	<i>s.d.</i>	<i>Mean</i>	<i>s.d.</i>	<i>Mean</i>	<i>s.d.</i>	<i>F</i>	<i>p</i>
Na-Me ^a	Vertical	109.17 ^a	7.34	107.71 ^a	7.24	107.65 ^a	7.24	107.65 ^a	7.28	4.83	0.014
Z-Ag (rt) ^b	Vertical	99.88 ^b	5.13	94.71 ^b	5.85	94.94 ^b	5.83	95.11 ^b	5.69	9.48	0.001
Z-Ag (lt) ^c	Vertical	98.47 ^c	4.97	94.92 ^c	5.46	94.86 ^c	5.65	94.79 ^c	5.58	6.37	0.005
Co-Go (rt)	Vertical	58.78	4.49	59.88	4.88	59.74	5.11	59.90	5.16	0.78	0.521
Co-Go (lt)	Vertical	58.08	4.64	58.36	4.49	58.50	4.82	58.56	4.64	0.55	0.658
Na-ANS ^d	Mid-Sagittal	46.29 ^d	3.18	45.93	2.99	45.85 ^d	3.05	45.84 ^d	3.15	2.8	0.074
ANS-PNS ^e	Mid-Sagittal	48.84 ^e	3.22	43.89 ^e	2.88	44.31 ^e	3.06	44.2 ^e	2.99	86.8	<.001
Na-A	Mid-Sagittal	51.12	3.59	50.69	3.26	50.94	3.97	50.81	3.76	0.88	<.001
Na-B	Mid-Sagittal	89.12	5.85	89.37	6.18	89.44	6.28	89.65	6.49	0.97	0.43

Table 8 (continued). Mean length (mm) and standard deviation (\pm s.d.) of Orthodontic Linear Dimensions for skulls compared to CBCT derived surface 3D renderings reconstructed from 153 (CBCT 10), 306 (CBCT 20) and 612 (CBCT 40) basis projections.

<i>Measurement</i>	<i>Axis</i>	<i>Modality</i>								<i>Significance</i>	
		<i>Skull</i>		<i>CBCT 10</i>		<i>CBCT 20</i>		<i>CBCT 40</i>			
		<i>Mean</i>	<i>s.d.</i>	<i>Mean</i>	<i>s.d.</i>	<i>Mean</i>	<i>s.d.</i>	<i>Mean</i>	<i>s.d.</i>	<i>F</i>	<i>p</i>
Go-Go	Coronal	90.92	8.16	88.37	5.47	88.38	5.57	88.37	5.64	1.27	0.32
Mental f. – Mental f. ^f	Coronal	46.45 ^f	3.96	45.67 ^f	4.59	45.91	4.5	45.55 ^f	3.11	8.96	0.001
Mo-Mo ^g	Coronal	19.45 ^g	2.16	22.67 ^g	1.75	22.89 ^g	1.59	22.87 ^g	2.13	40.68	<.001
Za-Za ^h	Coronal	121.78 ^h	6.13	119.07 ^h	5.93	119.03 ^h	6.06	119.11 ^h	6.09	17.57	<.001
NC-NC ⁱ	Coronal	24.82 ⁱ	1.52	23.64 ⁱ	1.4	23.39 ⁱ	1.41	23.68 ⁱ	1.46	17.69	<.001
Z-Z ^j	Coronal	94.37 ^j	3.28	93.76	3.35	93.69 ^j	3.42	93.59 ^j	3.37	4.85	0.014
J-J	Coronal	60.94	2.93	60.86	3.27	60.63	3.20	60.82	3.16	1.97	0.16

^aSkull dimensions greater than CBCT 10/20/40 (p=.006, p=.006, p=.005), ^{b,g,h}Skull dimensions greater than CBCT 10/20/40 (p<.001), ^cSkull dimensions greater than CBCT 10/20/40 (p=.002, p=.001, p=.001), ^dSkull dimensions greater than CBCT 20/40 (p=.044, p=.047), ^eSkull dimensions greater than CBCT 10/40 (p=.05, p=0), ^fSkull dimensions less than CBCT 10/20/40 (p<.001), ⁱSkull dimensions greater than CBCT 10/20/40 (p=0.002, p<.001, p<.001), ^jSkull dimensions greater than CBCT 20/40 (p=.02, p=.01)

CHAPTER V

DISCUSSION

Maxillofacial cone beam imaging provides clinicians with an opportunity to generate 3D volumetric renderings using relatively inexpensive third party personal computer based software. The availability of this technology will undoubtedly expand the use and application of 3D imaging in the field of orthodontics. However, while CBCT provides this facility at doses substantially lower than conventional CT, patient radiation dose is still several times higher than conventional cephalometric and panoramic digital imaging modalities. Appropriate selection of exposure settings (e.g. kVp, mAs) and adjustment of additional technical parameters is recommended to provide protocols aimed at minimizing patient dose. The aim of this study was to compare the reliability and accuracy of linear dimensions between common cephalometric landmarks on a sample of skulls to 3D measurements obtained from shaded surface 3D renderings reconstructed from CBCT datasets obtained from varying numbers of projection images.

While the reliability of measurements taken directly on skulls (mean absolute difference = $.45\text{mm} \pm .17\text{mm}$) was greater than those obtained from 3D renderings (range; $.77\text{mm}$ to $.88\text{mm}$), these are consistent with previously reported mean errors of less than 1mm [72,77].

For 3D measurements we found statistical differences between actual and virtual

linear measurements for 10 of the 16 dimensions. Relative percentage differences for most were less than 5%. For NC-NC and ANS-PNS, CBCT measurements underestimated actual dimensions by approximately 6% and 10% respectively. However for Mo-Mo, CBCT measurements overestimated actual dimensions by 17%. These specific measurement discrepancies may be attributed to interplay of numerous sources of variability. Statistical differences may have resulted from small standard deviations within the measurements. In addition, the greater intraobserver variability demonstrated by the 3D measurements may have also contributed. This is likely because the observer had to identify each landmark on the 3D rendering without the aid of a radiopaque fiducial reference. We believed that this task was a more representative simulation of the clinical situation and provides a combined assessment of inherent 3D landmark definition and identification error as well as error due to imaging procedure. [92] The segmentation process itself was customized for each skull and while not standardized, was adjusted to provide optimal “fill-in” when the volume was observed from various projections. Finally it is possible that the landmarks associated with the calculation of these linear dimensions have an inherent error due to landmark identification. While this source of variability and its clinical significance is well acknowledged in 2D cephalometry [92], the influence of this on 3D cephalometry is, as yet, unreported.

The most clinically important finding of this study was that there were no differences in accuracy between measurements obtained from 3D volumetric renderings no matter how many projection images were used to create the reconstruction. This is of clinical significance, particularly for CBCT units which use pulsed x-ray generators, because patient exposure will be directly related to the number of projection images

acquired. In this study 3D renderings produced using 153 basis projection images provided similar accuracy than those produced using 612. This represents a potential patient dose reduction of up to 75% and expels the concept that “more is better”.

There are numerous factors which should be considered when applying the results of this investigation to clinical situations. The accuracy of measurement distances between three dimensional landmarks on actual patients may be affected by a reduction in image quality due to soft-tissue attenuation, metallic artifacts and patient motion. There are also some potential limitations when using 3D images derived from CBCT data. Three dimensional volumetric depictions depend on appropriate segmentation – the thresholding of bone pixel values and suppression of surrounding tissue values to enhance the structure of interest. This process is dependent on the software algorithm, the spatial and contrast resolution of the scan, the thickness and degree of calcification or cortication of the bony structure and the technical skill of the operator. In this study, the Dolphin 3D software provides a semi-manual method of segmentation, dependent on the interaction of the operator with the data to produce a visually acceptable 3D rendering. These factors may, individually or in combination, result in deficiencies or voids in the surface of the volumetric rendering. These are most likely to occur in regions that are represented by few voxels or have gray values still representing bone, but outside the threshold. These areas include the posterior and anterior superior walls of the maxillary sinus, bone overlying the roots of the teeth and cortical bone of the mandibular condyle. Consequently this may lead to greater landmark identification error and subsequent measurement error.

Anatomic landmarks used in this study whose accuracy may be affected by poor

segmentation include Mo, A point, ANS, PNS and Mental f. In addition, the method of establishing dimensional truth could have potentially contributed to bias in the results. While the landmark identification and measurements on the 3D rendered images were repeated three times by a single observer, the landmark identification on the skulls was performed only once and measurements performed independently three times by consensus of two observers. This reduced the error of point identification on the skulls; however, the establishment of a consensus landmark location was necessary to provide a fiducial reference to which we could assess the inherent clinical inaccuracies of both landmark identification and measurement associated with the 3D image rendering.

Based on the comparable accuracy of dimensions obtained from 3D rendered images reconstructed using the lowest number of projection images, it is unwise to interpret the findings of this study as advocating the use of CBCT in general orthodontic practice. Our study does not take into account the overall comparative radiation detriment required to produce such images nor the clinical efficacy of the technique compared to conventional imaging. We do however advocate clinical cost/benefit analyses incorporating exposure considerations to assist in developing appropriate patient selection criteria for the use of CBCT in cephalometric imaging.

CHAPTER VI

SUMMARY AND CONCLUSIONS

- Linear measurements on 3D shaded surface renderings from CBCT datasets using commercial cephalometric analysis software have variable accuracy perhaps due to difficulty in assigning points precisely using 3D radiographic images. This problem was not encountered in measuring “anatomic truth” as the consensus points were marked on the skulls using pencil. Hence variability could be a factor of the inaccuracy of the human in determining unmarked points.
- Reducing the number of image projections needed to construct a 3D shaded surface rendering does not result in reduced dimensional accuracy of 3D measurements and potentially provides reduced patient radiation exposure.

REFERENCES

1. Schulze D, Heiland M, Thurmann H, Adam G. *Radiation exposure during midfacial imaging using 4- and 16-slice computed tomography, cone beam computed tomography systems and conventional radiography*. Dentomaxillofac Radiol 2004;33:83-86.
2. Ludlow JB, Davies-Ludlow LE, Brooks SL. *Dosimetry of two extraoral direct digital imaging devices: NewTom cone beam CT and Orthophos Plus DS panoramic unit*. Dentomaxillofac Radiol 2003;32:229–243.
3. Mah JK, Danforth RA, Bumann A, Hatcher D. *Radiation absorbed in maxillofacial imaging with a new dental computed tomography device*. Oral Surg Oral Med Oral Pathol Oral Radiol Endod 2003;96:508–513.
4. Tsiklakis K, Donta C, Gavala S, Karayianni K, Kamenopoulou V, Hourdakakis CJ. *Dose reduction in maxillofacial imaging using low dose Cone Beam CT*. Eur J Radiol. 2005 Jun 21.
5. Swennen GRJ, Schutyser F. *Three-dimensional cephalometry: Spiral multi-slice vs cone-beam computed tomography*. Am J Orthod Dentofacial Orthop 2006;130:410-416.
6. Farman AG, Jacobs W. *Digital options for panoramic radiology*. Panoramic Imaging News 2003;3(4):1-6.
7. Schulze RKW, Burkhardt Gloede M, Doll GM. *Landmark identification on direct digital versus film-based cephalometric radiographs: A human skull study*. Am J Orthod Dentofacial Orthop 2002; 122:635-642.
8. Farman AG, Farman TT. *Extraoral and panoramic systems*. Dental Clinics of North America 2000;44:257-272.
9. Gregston M, Kula T, Hardman P, Glaros A, Kula K. *A comparison of conventional and digital radiographic methods and cephalometric analysis software: I. Hard tissue*. Semin Orthod 2004;10:204-211.

10. Kublashvili T, Kula K, Glaros A, Hardman P, Kula T. *A Comparison of Conventional and Digital Radiographic Methods and Cephalometric Analysis Software: II. Soft Tissue*. Semin Orthod 2004;10:212-219.
11. Malkoc S, Sari Z, Usumez S, Koyuturk AE. *The effect of head rotation on cephalometric radiographs*. Eur J Orthod. 2005 Jun;27(3):315-21.
12. Major P, Johnson D, Hesse K, Glover K 1994 *Landmark identification error in posterior anterior cephalometrics*. Angle Orthod. 1994;64: 447–454.
13. Major P, Johnson D, Hesse K, Glover K. *Effect of head orientation on posterior anterior cephalometric landmark identification*. Angle Orthod. 1996;66: 51–60.
14. Farman AG, Farman TT. *A comparison of image characteristics and convenience in panoramic radiography using charge-coupled device, storage phosphor, and film receptors*. J Digit Imaging. 2001;14(Suppl 1): 48-51.
15. Korner M, Weber CH, Wirth S, Pfeifer KJ, Reiser MF, Treitl M. *Advances in Digital Radiography: Physical Principles and System Overview*. Radiographics 2007;27:675-686.
16. “Quantum Efficiency.” McGraw-Hill Dictionary of Scientific and Technical Terms. McGraw-Hill Companies, Inc., 2003. *Answers.com* 03 Jun. 2007. <http://www.answers.com/topic/quantum-efficiency>
17. Hatcher, D.C. and C.L. Aboudara. *Diagnosis goes digital*. Am J Orthod Dentofacial Orthop 2004;125:512-515.
18. Mozzo P, Procacci C, Tacconi A, Martini PT, Andreis IA. *A new volumetric CT machine for dental imaging based on the cone-beam technique: preliminary results*. Eur Radiol 1998;8:1558–1564.
19. Farman AG, Levato C, Scarfe WC. *A primer on cone beam CT*. Inside Dentistry 2007(Jan):90-93.
20. Hashimoto K, Arai Y, Iwai K, Araki M, Kawashima S, Terakado M. *A comparison of a new limited cone beam computed tomography machine for dental use with a multidetector row helical CT machine*. Oral Surg Oral Med Oral Pathol Oral Radiol Endod 2003;95:371–377.
21. Sukovic P. *Cone beam computed tomography in craniofacial imaging*. Orthod Craniofac Res 2003;6(Suppl 1):31–36.
22. Baba R, Ueda K, Okabe M. *Using a flat-panel detector in high resolution cone beam CT for dental imaging*. Dentomaxillofac Radiol 2004;33:285-290.

23. Hollender, LG. *Controversies in Oral and Maxillofacial Surgery*, ed. E.J. Worthington P. 1994, Philadelphia: WB Saunders. pp.1-12.
24. Kjellberg H, Ekestubbe A, Kiliaridis S, Thilander B. *Condylar height on panoramic radiographs. A methodologic study with a clinical application*. Acta Odontol Scand. 1994. 52(1): p. 43-50.
25. Katzberg, RW. *State of the art: Temporomandibular joint imaging*. Ann Roy Aust Coll Dent Surg 1989;10:32-52.
26. Seligman D, Okeson , *Orthodontics Occlusion and Temporomandibular Disorders*. In: Orthodontics and Dentofacial Orthopedics, J. McNamara and W. Brudon, Editors. 2001, Needham Press: Ann Arbor. pp. 519-543.
27. Kitai N, Kreiborg S, Bakke M, Paulsen HU, Moller E, Darvann TA, Pedersen H, Takada K. *Three-dimensional magnetic resonance image of the mandible and masticatory muscles in a case of juvenile chronic arthritis treated with the Herbst appliance*. Angle Orthod 2002;72(1):p. 81-87.
28. Blackwood HJ. *Arthritis of the mandibular joint*. Br Dent J 1963;115:317-326.
29. Proffit WR. *Treatment planning: the search for wisdom*. In: Surgical Orthodontic Treatment, Proffit WR, Editor. 1991, Mosby-Year Book: St. Louis. pp. 158-159.
30. Ong TK, Franklin CD. *A clinical and histopathological study of osteoarthritis of the temporomandibular joint*. Br J Oral Maxillofac Surg 1996;34:186-192.
31. Dahlstrom L, Lindvall AM. *Assessment of temporomandibular joint disease by panoramic radiography: reliability and validity in relation to tomography*. Dentomaxillofac Radiol 1996; 25:197-201.
32. Winter A. *NewTom 9000 Accuracy*. 2000. Accessed June 4, 2007 <http://www.endomail.com/articles/aw01newtom.html>
33. Ruf S, Pancherz H. *Is orthopantomography reliable for TMJ diagnosis? An experimental study on a dry skull*. J Orofac Pain 1995;9:365-374.
34. Ziegler CM, Woertcher R, Brief J, Hassfeld S. *Clinical indications for digital volume tomography in oral and maxillofacial surgery*. Dentomaxillofac Radiol 2002;31:126–130.
35. Nakagawa Y, Kobayashi K, Ishii H, Mishima A, Ishii H, Asada K, Ishibashi K. *Preoperative application of limited cone beam computerized tomography as an assessment tool before minor oral surgery*. Int J Oral Maxillofac Surg. 2002;31:322-326.

36. Danforth RA, Peck J, Hall P. *Cone beam volume tomography: an imaging option for diagnosis of complex mandibular third molar anatomical relationships*. J Calif Dent Assoc 2003;31:847-852.
37. Heiland M, Schmelzle R, Hebecker A, Schulze D. *Intra-operative 3D imaging of the facial skeleton using the SIREMOBIL Iso-C3D*. Dentomaxillofac Radiol. 2004;33:130-132.
38. Hamada Y, Kondoh T, Noguchi K, Iino M, Isono H, Ishii H, Mishima A, Kobayashi K, Seto K. *Application of limited cone beam computed tomography to clinical assessment of alveolar bone grafting: a preliminary report*. Cleft Palate Craniofac J 2005;42:128-137.
39. Hatcher DC, Dial C, Mayorga C. *Cone beam CT for pre-surgical assessment of implant sites*. J Calif Dent Assoc 2003;31:825-833.
40. Sarment DP, Sukovic P, Clinthorne N. *Accuracy of implant placement with a stereolithographic surgical guide*. Int J Oral Maxillofac Implants 2003;18:571-577.
41. Sato S, Arai Y, Shinoda K, Ito K. *Clinical application of a new cone-beam computerized tomography system to assess multiple two-dimensional images for the preoperative treatment planning of maxillary implants: case reports*. Quintessence Int 2004;35:525-528.
42. Kobayashi K, Shimoda S, Nakagawa Y, Yamamoto A. *Accuracy in measurement of distance using limited cone-beam computerized tomography*. Int J Oral Maxillofac Implants 2004;19:228-231.
43. Mah JD, Hatcher D. *Current status and future needs in craniofacial imaging*. Orthod Craniofac Res 2003;6(Suppl 1):10-16.
44. Vannier MW. *Craniofacial computed tomography scanning: technology, applications and future trends*. Orthod Craniofac Res 2003;6(Suppl 1):23-30.
45. Maki K, Inou N, Takanishi A, Miller AJ. *Computer-assisted simulations in orthodontic diagnosis and the application of a new cone beam X-ray computed tomography*. Orthod Craniofac Res 2003;6(Suppl 1):95-101.
46. Baumrind S, Carlson S, Beers A, Curry S, Norris K, Boyd RL. *Using three-dimensional imaging to assess treatment outcomes in orthodontics: a progress report from the University of the Pacific*. Orthod Craniofac Res 2003;6(Suppl 1):132-142.

47. Aboudara CA, Hatcher D, Nielsen IL, Miller A. *A three-dimensional evaluation of the upper airway in adolescents*. Orthod Craniofac Res 2003;6(Suppl 1):173-17.
48. Danforth RA, Dus I, Mah J. 3-D volume imaging for dentistry: a new dimension. J Calif Dent Assoc 2003;31:817-823.
49. Lascala CA, Panella J, Marques MM. *Analysis of the accuracy of linear measurements obtained by cone beam computed tomography (CBCT-NewTom)*. Dentomaxillofac Radiol 2004;33:291-294.
50. Bianchi S, Anglesio S, Castellano S, Rizzi L, Ragona R. *Absorbed doses and risk in implant planning: comparison between spiral CT and cone-beam CT*. Dentomaxillofac Radiol 2001;30(Suppl 1):S28.
51. Halazonetis DJ. *From 2-dimensional cephalograms to 3-dimensional computed tomography scans*. Am J Orthod Dentofacial Orthop 2005; 127:627-637.
52. Ngan DC, Kharbanda OP, Geenty JP, Darendeliler MA. *Comparison of radiation levels from computed tomography and conventional dental radiographs*. Aust Orthod J 2003;19:67-75.
53. Dus I. *The Next "Revolution."* American Association of Dental Maxillofacial Radiographic Technicians.
http://www.aadmrt.com/static.aspx?content=currents/Dus_fall03 accessed Nov. 30, 2004
54. Hilgers ML, Scarfe WC, Scheetz JP, Farman AG. *Accuracy of linear TMJ measurements with cone beam computed tomography and digital cephalometric radiography*. Am J Orthod Dentofacial Orthop 2005;127:803-811.
55. Hajeer MY, Millett DT, Ayoub AF, Siebert JP. *Current products and practices. Applications of 3D imaging in orthodontics: Part I*. J of Orthod 2004;31:62-70
56. Largravere MO, Major PW. *Proposed reference point for 3-dimensional cephalometric analysis with cone-beam computerized tomography*. Am J Orthod Dentofacial Orthop 2005;128:657-660.
57. Major PW, Johnson DE, Hesse KL, Glover KE. *Landmark identification error in posterior anterior cephalometrics*. Angle Orthod 1994;64:447-454.
58. Athanasiou AE. *Orthodontic cephalometry*. London and Baltimore: Mosby-Wolfe; 1995.

59. Park SH, Yu HS, Kim KD, Lee KJ, Baik HS. *A proposal for a new analysis of craniofacial morphology by 3-dimensional computed tomography*. Am J Orthod Dentofacial Orthop. 2006;129:600.e23-3442.
60. Broadbent BH Sr, Broadbent BH Jr, Golden WH. *Bolton standards of dentofacial developmental growth*. St Louis: Mosby; 1975.
61. Baumrind S, Moffitt FH, Curry S. *The geometry of three-dimensional measurement from paired coplanar x-ray images*. Am J Orthod 1983;84:313-322.
62. Grayson BH, McCarthy JG, Bookstein F. *Analysis of craniofacial asymmetry by multiplane cephalometry*. Am J Orthod 1983;84:217-224.
63. Grayson BH, LaBatto FA, Kolber AB, McCarthy JG. *Basilar multiplane cephalometric analysis*. Am J Orthod 1985;88:503-516.
64. Trocme MC, Sather AH, An KN. *A biplanar cephalometric stereoradiography technique*. Am J Orthod Dentofacial Orthop 1990;98:168-175.
65. Farman AG, Scarfe WC. *Development of imaging selection criteria and procedures should precede cephalometric assessment with cone-beam computed tomography*. Am J Orthod 2006;130:257-265.
66. Moshiri M, Scarfe WC, Hilgers ML, Scheetz JP, Silveira AM, Farman AG. *Accuracy of linear measurements from imaging plate and CBCT-derived lateral cephalometric images*. Am J Orthod Dentofacial Orthop. 2007;(In press: manuscript # AJODO-D-06-00173R1)
67. Adams GL, Hatcher DC, Miller AJ. *Comparison between traditional two-dimensional cephalometry and a three-dimensional approach*. Division of Orthodontics. University of California. San Francisco, AJODO. Abstract, Vol. 22, Number 1, Page 117, July 2002
68. Chidiac JJ, Shofer FS, Al-Kutoub A, Laster LL, Ghafari J. *Comparison of CT scanograms and cephalometric radiographs in craniofacial imaging*. Orthod Craniofac Res 2002;5:104-13.
69. Chan G, Palomo JM, Baden S, Hans MG. *Accuracy and reliability of cephalometric and CBCT linear measurements*. J Dent Res 86(Spec Iss B):abstract #0770, 2007.
70. Lagravere MO, Hansen L, Harzer W, Major PW. *Plane orientation for standardization in 3-dimensional cephalometric analysis with computerized tomography imaging*. Am J Orthod Dentofacial Orthop 2006;129:601-604.

71. Hildebolt CF, Vannier MW, Knapp RH. *Validation study of skull three-dimensional computerized tomography measurements*. Am J Phys Anthropol 1990;82:283-294.
72. Kragstov J, Bosch C, Gyldensted C, Sindet-Pedersen S. *Comparison of the reliability of craniofacial anatomic landmarks based on cephalometric radiographs and three-dimensional CT scans*. Cleft Palate Craniofac J 1997;34:111-116
73. Nagashima M, Inoue K, Sasaki T, Miyasaka K, Matsumura G, Kodama G. *Three-dimensional imaging and osteometry of adult human skulls using helical computed tomography*. Surg Radiol Anat 1998;20:291-297.
74. Cavalcanti MG, Rocha SS, Vannier MW. *Craniofacial measurements based on 3D-CT volume rendering: implications for clinical applications*. Dentomaxillofac Radiol. 2004;33:170-176.
75. Cavalcanti MG, Vannier MW. *Quantitative analysis of spiral computed tomography for craniofacial clinical applications*. Dentomaxillofac Radiol. 1998;27:344-350.
76. Jung H, Kim HJ, Kim DO, Hong SI, Jeong HK, Kim KD, Kim Y, Yoo S, Yoo H. *Quantitative analysis of three-dimensional rendered imaging of the human skull acquired from multi-detector row computed tomography*. J Digit Imaging. 2002;15:232-239.
77. Cavalcanti MG, Haller JW, Vannier MW. *Three-dimensional computed tomography landmark measurement in craniofacial surgical planning: experimental validation in vitro*. J Oral Maxillofac Surg 1999;57:690-694.
78. Williams FL, Richtsmeier JT. *Comparison of mandibular landmarks from computed tomography and 3D digitizer data*. Clin Anat. 2003;16:494-500.
79. Cavalcanti MGP, Ruprecht A, Vannier MW. *3D volume rendering using multislice computed tomography for dental implants*. Dentomaxillofac Radiol 2002;31:218-223.
80. Swennen GRJ, Schutyser F. *Three-dimensional cephalometry: Spiral multi-slice vs cone-beam computed tomography*. Am J Orthod Dentofacial Orthop 2006;130:410-416.
81. Swennen GRJ. *Three dimensional cephalometric reference system*. In: Swennen GRJ, Schutyser F, Hausamen JE, editors. Three dimensional cephalometry. A color atlas and manual. Heidelberg: Springer; 2005. p.94-112.

82. Swennen GRJ, Schutyser F, Barth EL, De Groeve P, De Mey A. *A new method of 3-D cephalometry. Part I: the anatomic Cartesian 3-D reference system.* J Craniofac Surg 2006;17:314-325.
83. Swennen GRJ. *Three dimensional cephalometric soft tissue landmarks.* In: Swenen GRJ, Schutyser F, Hausamen JE, editors. Three dimensional cephalometry. A color atlas and manual. Heidelberg: Springer; 2005. p.116-181.
84. Swennen GRJ. *Three dimensional cephalometric soft tissue landmarks.* In: Swenen GRJ, Schutyser F, Hausamen JE, editors. Three dimensional cephalometry. A color atlas and manual. Heidelberg: Springer; 2005. p.186-226.
85. Swennen GRJ, Barth EL, Schutyser F, De Groeve P, Lemaitre A. *Three-dimensional (3-D) cephalometry, the basics for virtual planning.* J Cranio Maxillofac Surg 2004;32(Suppl 1):135.
86. Feldkamp LA, Davis LC, Kress JW. *Practical conebeam algorithm.* J Opt Soc Am 1984;1:612-619.
87. Geelen W, Wenzel A, Gotfredsen E, Kruger M, Hansson LG. *Reproducibility of cephalometric landmarks on conventional film, hardcopy, and monitor-displayed images obtained by the storage phosphor technique.* Eur J Orthod. 1998;20:331-40
88. Tsao DH, Kazanoglu A, McCasland JP. *Measurability of radiographic images.* Am J Orthod. 1983;84:212-6.
89. Ludlow JB, Davies-Ludlow LE, Brooks SL, Howerton WB. *Dosimetry of 3 CBCT devices for oral and maxillofacial radiology: CB Mercuray, NewTom 3G and i-CAT.* Dentomaxillofac Radiol. 2006;35(4):219-26.
90. Gijbels F, Sanderink G, Wyatt J, Van Dam J, Nowak B, Jacobs R. *Radiation doses of indirect and direct digital cephalometric radiography.* British Dental Journal. 2004;197(3):149-52.
91. Kusnoto B, Evans CA, BeGole EA, De Rijk W. *Assessment of 3-dimensional computer-generated cephalometric measurements.* Am J Orthod Dentofacial Orthop 1999;116:390-9
92. Kamoen A, Dermaut L, Verbeeck R. *The clinical significance of error measurement in the interpretation of treatment results.* Eur J Orthod. 2001;23:569-578.

CURRICULUM VITAE

NAME: April A. Brown

ADDRESS: 1715 Somerset Pl Apt 6
Louisville, KY 40220

DOB: Hope, Arkansas – February 26, 1983

EDUCATION & TRAINING:

B.S., Biology
Ouachita Baptist University
2001-2004

D.M.D.
University of Louisville School of Dentistry
2004-2008

AWARDS: Ouachita Baptist University

- Arkansas Governor's Scholar
- OBU Trustee Scholarship
- OBU President's List (all semesters attended)
- Best Buy Award
- Discover Card Scholarship
- Temple-Inland Award

University of Louisville School of Dentistry

- Dean's Scholar
- Dean's List
- Honors Student in Histology
- Top 10% of Students in Gross Anatomy
- Top 10% of Students in Pharmacology
- Second Place Award in Research Louisville 2007

PROFESSIONAL
SOCIETIES:

- Alpha Chi Honor Society
- Louisville American Student Dental Association.
- Alpha Omega
- Christian Medical and Dental Association

PUBLICATIONS:

- University of Louisville School of Dentistry
 - As Principal Investigator
Brown A, Scarfe WC, Moshiri M, Scheetz JP, Silveira AM, Farman A. *Linear Accuracy of Cone Beam CT-Derived 3D Images*. The Angle Orthod. [In press: March 2008].
 - As Research Associate
Moshiri M, Scarfe WC, Hilgers MJ, Scheetz JP, Silveira AM, Farman A. *Accuracy of Linear Measurements From Imaging Plate and CBCT-derived Lateral Cephalometric Images*. American Journal of Orthodontics and Orthopedics Oct. 2007